

# Importance of Low-Angle Grain Boundaries in $\text{YBa}_2\text{Cu}_3\text{O}_{7-\delta}$ Coated Conductors

J. H. Durrell<sup>§</sup> and N. A. Rutter

Department of Materials Science and Metallurgy, University of Cambridge, Cambridge CB2 3QZ

**Abstract.** Over the past ten years the perception of grain boundaries in  $\text{YBa}_2\text{Cu}_3\text{O}_{7-\delta}$  conductors has changed greatly. They are no longer a problem to be eliminated but an inevitable and potentially favourable part of the material. This change has arisen as a consequence of new manufacturing techniques which result in excellent grain alignment, reducing the spread of grain boundary misorientation angles. At the same time there is considerable recent evidence which indicates that the variation of properties of grain boundaries with mismatch angle is more complex than a simple exponential decrease in critical current. This is due to the fact that low-angle grain boundaries represent a qualitatively different system to high angle boundaries. The time is therefore right for a targeted review of research into low-angle  $\text{YBa}_2\text{Cu}_3\text{O}_{7-\delta}$  grain boundaries. This article does not purport to be a comprehensive review of the physics of grain boundaries as found in  $\text{YBa}_2\text{Cu}_3\text{O}_{7-\delta}$  in general; for a broader overview we would recommend that the reader consult the comprehensive review of Hilgenkamp and Mannhart (Rev. Mod. Phys., **74**, 485, 2002). The purpose of this article is to review the origin and properties of the low-angle grain boundaries found in  $\text{YBa}_2\text{Cu}_3\text{O}_{7-\delta}$  coated conductors both individually and as a collective system.

## 1. Introduction

The cuprate superconductor  $\text{YBa}_2\text{Cu}_3\text{O}_{7-\delta}$  has properties which suggest that it would make an excellent material for practical superconducting applications. It combines a large upper critical field, a critical temperature well above 77 K and the potential for very high critical currents if suitable pinning centres are present[1][2]. Early on in the exploration of the properties of this material it was discovered that, while these attributes were found in thin films grown on single-crystal substrates[3], the presence of grain boundaries in polycrystalline samples causes a large reduction in the overall critical current density ( $J_C$ ) †. It became apparent that this was due to the fact that the critical current density of individual grain boundaries falls off rapidly with increasing misorientation angle ( $\theta_{gb}$ ) [4, 5, 6]. Consequently, while good quality material could be made using thin film growth techniques onto single-crystal substrates the limited substrate size meant that long conductor lengths were initially unachievable. Naturally this observation resulted in a considerable research effort into understanding the properties of these grain boundaries. Essentially  $\text{YBa}_2\text{Cu}_3\text{O}_{7-\delta}$  grain boundaries, and those in the very similar superconducting materials where Y is replaced with another rare earth (RE) such as Nd or Dy with the generic formula  $\text{REBa}_2\text{Cu}_3\text{O}_{7-\delta}$ , may be divided into two categories depending on the nature of the coupling of the order

<sup>§</sup> To whom correspondence should be addressed (jhd25@cam.ac.uk)

† The uppercase symbol  $J$  is used to represent a macroscopic current density whilst the lowercase  $j$  represents the local microscopic current density within a grain or crossing a grain boundary.

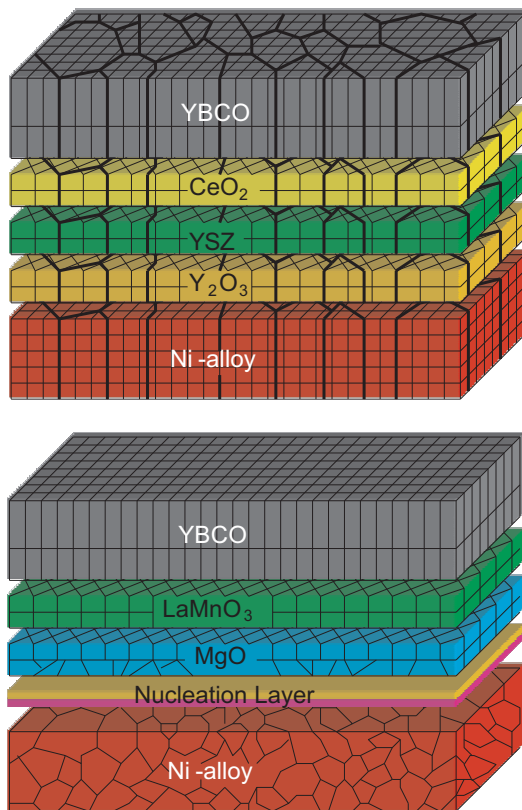


**Figure 1.** A schematic of the structure of RABiTS (top) and IBAD (bottom) conductors. The particular layer materials shown here are examples and there are many variations. Note that in the RABiTS material the alignment arises from the metal tape material whereas in IBAD the orientation is imparted by the aligned MgO layer.

parameter across the boundary [7]. For grain boundaries which have misorientation angles larger than about ten degrees there is a continuous disordered layer along the boundary, the superconducting order parameter is discontinuous and the grain boundary is a Josephson junction. For smaller misorientation angles however, the grain boundary may be modelled as a series of dislocation cores with regions of strained material between them. While the strain affects the superconducting properties the order parameter is continuous and the critical current properties may be described in terms of the pinning of vortex lines, as in the intra-grain regions. This prompted research into how to ameliorate the deleterious effect of strain at boundaries, one notable example being the use of Ca-doping [8].

In fact, the breakthrough that made possible  $\text{YBa}_2\text{Cu}_3\text{O}_{7-\delta}$  coated conductors was not achieved through the control of single grain boundaries, but by the development of techniques which allow the manufacture of long-length conductors in which the superconducting grains have orientations which are well aligned. Two broad classes of technique have been developed, both aim to provide a method of creating a flexible template which, while not entirely single-crystalline, allows control over grain boundary angles. One class of technique involves depositing an aligned seed layer onto an unoriented substrate, either by using the preferential removal of unwanted orientations with an ion beam, or by depositing at an angle which encourages a preferential orientation[9, 10]. The other class involves

the biaxial texturing of a metallic substrate coupled with the heteroepitaxial growth of a buffer layer system[12]. It is instructive to note that while these two techniques are quite different they have both resulted in competitive commercial materials [13, 14]. The modern  $\text{YBa}_2\text{Cu}_3\text{O}_{7-\delta}$ -based coated conductors owe their performance to this achievement of control of the disposition and angle of grain boundaries. Crucially the relatively small grain boundary angles found in these pseudo-single-crystal materials results in an interesting set of superconducting properties. The grain boundary angles are small enough that the physical properties of the overall conductor are not exclusively dominated by the grain boundaries present in the material. This is due to the fact that the critical current of these "low-angle" grain boundaries can tend to that of the intra-grain under several conditions, depending on temperature, field magnitude, orientation and potentially grain boundary doping.

As individual grain boundaries have complex properties, consequently the behaviour of the final coated conductor product is equally a complex function of the grain and grain boundary properties. Moreover the form of the grain boundaries themselves can be strongly influenced by the technique used to deposit the  $\text{YBa}_2\text{Cu}_3\text{O}_{7-\delta}$  overlayer, varying from an almost planar frontier to those which follow a highly convoluted path through the material in positions which are only weakly dependent on the location of the grain boundaries in the underlying template grain [15]. Finally, emancipation from the tyranny of the grain boundary has led to a resurgence of interest in the traditional route to enhancing critical currents, that of introducing more (and better) pinning sites to hold the vortex lines in place [2]. However, there is interplay between intra-grain (IG) and grain boundary (GB) properties and the overall critical current of a conductor is always determined by the weakest link. Consequently enhancement of intra-grain properties can lead to the grain boundary properties again limiting the measured critical current.

We aim in this review to describe the present state of understanding of the nature and properties of low-angle grain boundaries in  $\text{YBa}_2\text{Cu}_3\text{O}_{7-\delta}$  and relate this to the properties of coated conductors. We contend that further enhancement of coated conductor properties requires a coherent picture where understanding of growth is coupled to an appreciation of the properties of single grain boundaries and an understanding of how these interact to give rise to the behaviour of the entire coated conductor. We divide the body of this review into four sections; the origins of grain boundaries in coated conductors and how their number, nature and type is dependent on conductor preparation route; a review of the nature and properties of single grain boundaries; a review of experimental evidence of how grain boundaries affect the critical current properties of conductors and finally how such systems may be studied by the modelling of grain boundary networks.

## 2. The Microstructural Nature of Grains and Grain Boundaries in Coated Conductors

Coated conductor technology has developed using a wide range of different fabrication techniques. The nature of grain boundaries varies widely between different types of coated conductor, depending not only on the route used to produce the  $\text{YBa}_2\text{Cu}_3\text{O}_{7-\delta}$  film, but also on the types of buffer layers and metallic substrates used. The main features of the grain boundary network which are of importance in determining the electrical properties of a coated conductor can be summarised as:

- grain size - which determines the number and extent of grain boundaries in the sample;
- grain shape - whether they are equiaxed or elongated;
- the misorientations between adjacent grains;
- the morphology of the boundaries - whether they meander or are planar in form;

- uniformity of the microstructure through the superconductor film thickness

This section will describe how the more popular coated conductor fabrication routes determine these important features.

### 2.1. Deformation-Textured Substrates

Here, we focus on the route commonly known as the Rolling-Assisted Biaxially Textured Substrate (RABiTS) method, in which a metallic tape containing grains with preferred crystallographic alignments is used as the base substrate as shown in the upper half of figure 1. Alignment of the superconducting film is achieved through heteroepitaxial growth of subsequent layers onto the textured substrate and hence many features of the grain boundaries in the  $\text{YBa}_2\text{Cu}_3\text{O}_{7-\delta}$  layer are influenced by the grain structure of the metallic substrate.

Commonly, a Ni-based alloy is used as the substrate. Amongst many advantages of Ni for this application, a property of crucial importance when considering grain boundary networks is that a preferential crystallographic texture can be generated via rolling and recrystallisation. In order to deposit a superconductor, such as  $\text{YBa}_2\text{Cu}_3\text{O}_{7-\delta}$ , with the desired orientation a suitable texture for substrate materials is the cube texture  $\{100\} \langle 001 \rangle$ . Whilst it is possible to control to some extent both the size and the shape [16] of the grains in a Ni-based alloy, a more important factor is the spread of orientations about the ideal cube texture [17, 18, 19, 20]. The extent of texture of a RABiTS tape is typically characterised by the measurement of the Full-Width at Half-Maximum (FWHM) of X-Ray rocking curves and phi-scans. It is important to note that these simply give an overall, global representation of the grain orientations and give no indication of whether there may be any angular correlation between grains which are spatially adjacent [21]. Typical values in Ni-W substrates are 5-7° for the out-of-plane FWHM and 4-6° for the true in-plane FWHM [22]. It is important to note that the FWHM of a phi-scan is not a direct measurement of the in-plane grain orientations, but a combination of both in-plane and out-of-plane rotational deviations from the ideal texture [23].

Buffer layers deposited onto these substrates are typically oxides such as  $\text{CeO}_2$ , YSZ and  $\text{Y}_2\text{O}_3$ . The aim is to reproduce the texture of the underlying substrate, and in fact it is commonly observed that the grain alignments actually improve, with reductions in the FWHM by as much as 1°. Hence the morphology (i.e. shapes and sizes) of grains in the buffer layers usually reproduces that found in the substrate, though the texture can be somewhat sharper.

Detailed spatial and angular information regarding the relationship between the grain networks in substrates and buffer layers has been gathered using Electron Back-Scatter Diffraction (EBSD) [24, 17, 21] and microdiffraction [25]. EBSD measurements have not generally shown significant angular correlation between adjacent grains in the substrate tapes and hence grain boundary angles are approximately as would be predicted from the macroscopic texture [26]. EBSD measurements on substrates and buffer layer films tend to show smaller grain boundary angles in the buffer layer film, confirming the slight improvement in texture of the film [21]. Microdiffraction has the advantage of being able to probe both substrate and film simultaneously and such experiments clearly demonstrate this reduction in grain misalignment [25]. Furthermore, the technique has shown that the greatest improvement is in buffer layer grains deposited on significantly misoriented substrate grains. The mechanism for this is that  $\text{CeO}_2$  growing on a Ni template grain will grow in an orientation such that the direction of the  $c$ -axis of the film is intermediate between the  $c$ -axis of the underlying Ni grain and the surface normal, which would lead to an improvement in the out-of plane texture, but no change of in-plane texture. This was also seen in the EBSD measurements carried out by Feldmann et al. [27, 28] who were able to look at the same region

of a sample by milling away subsequent thin layers. These measurements clearly demonstrate an improvement in out-of-plane alignment, but little change in the in-plane orientations of the grains.

*2.1.1. PLD on RABiTS* Pulsed-Laser Deposition (PLD) has been used widely during coated conductor development and serves a useful purpose in the study of model systems which enable research into the nature of grain boundaries. X-Ray diffraction measurements[29, 23] of  $\text{YBa}_2\text{Cu}_3\text{O}_{7-\delta}$  films deposited by PLD indicate epitaxial growth with the texture of the underlying film being reproduced or even slightly improved upon such that  $\text{YBa}_2\text{Cu}_3\text{O}_{7-\delta}$  layers commonly exhibit misorientations with FWHM of around  $4^\circ$  out-of-plane and  $5^\circ$  in-plane. EBSD studies generally indicate that the grain structure of the underlying layer is reproduced in a  $\text{YBa}_2\text{Cu}_3\text{O}_{7-\delta}$  overlayer deposited by PLD [30, 31, 24, 27].

The fact that the grain boundary network is important in determining the electromagnetic properties of coated conductor films has been well-demonstrated using both Magneto-Optical (MO) imaging measurements and light microscopy [32, 24, 1]. Visualisation of areas of magnetic flux penetration indicate that dissipation occurs at regions which match up to the grain boundaries in the substrate (identified by etching the  $\text{YBa}_2\text{Cu}_3\text{O}_{7-\delta}$  film), again indicating that the boundaries in the  $\text{YBa}_2\text{Cu}_3\text{O}_{7-\delta}$  match up with those in the substrate and buffers[24].

It has been observed that above a single template grain of the Ni-based substrate, the  $\text{YBa}_2\text{Cu}_3\text{O}_{7-\delta}$  exhibits a mosaic structure[31]. As the  $\text{YBa}_2\text{Cu}_3\text{O}_{7-\delta}$  grows via columnar growth, these sub-grains, whilst being influenced by the underlying grain, nucleate and grow with slightly different orientations. Further convincing evidence of a mosaic  $\text{YBa}_2\text{Cu}_3\text{O}_{7-\delta}$  sub-grain structure above each template grain comes from transmission electron microscopy (TEM) measurements [33], which show that the sub grains can range in lateral size from  $0.2\text{-}2\ \mu\text{m}$  and have an angular spread of up to around  $3^\circ$ . This work showed no correlation between the nature of the sub-grain structure and the orientation of the underlying template grain.

The most detailed study of the evolution of the grain boundary structure from substrate to superconductor is that of Feldmann et al.[27] This work has shown that the spatial and orientational structure of grains is preserved from the buffer layer into the superconductor, at least up to  $0.65\ \mu\text{m}$  from the base of a  $0.65\ \mu\text{m}$ -thick film. No evidence of a sub-grain structure was observed in this work.

As detailed in the previous section, the current carrying capability of the grains is also important. PLD has been known for some time to produce films with significant flux pinning (especially when compared with  $\text{YBa}_2\text{Cu}_3\text{O}_{7-\delta}$  single crystals) due to the large defect density. However it has been shown that the extent of flux pinning can be enhanced by intentionally introducing nanoscale particles of a second phase which can act to pin magnetic flux lines [34, 35, 36].

Early results with PLD found that this technique produced films which were inhomogeneous through the thickness of the superconductor[37]. Thicker films (around  $2\ \mu\text{m}$ ) showed the presence of randomly oriented material as well as  $a$ -axis grains, leading to rather poor  $J_C$  values. In addition there were problems at the superconductor/buffer interface with the formation of additional, non-superconducting phases. In thin films ( $0.2\ \mu\text{m}$ ) however, TEM studies showed columnar growth of well oriented  $c$ -axis  $\text{YBa}_2\text{Cu}_3\text{O}_{7-\delta}$  grains extending throughout the thickness [27]. Above any single template grain there are a number of sub-grains, though these display negligible relative crystallographic misorientation and are distinguishable only due to the fact they are separated by anti-phase boundaries. With improved buffer layers, PLD has successfully been used to prepare more uniform

YBa<sub>2</sub>Cu<sub>3</sub>O<sub>7-δ</sub> layers such that the grain boundary network is more closely matched to that of the underlying template[29], though TEM measurements still show the existence of second phase particles and pores, indicating that the issue of current flow within grains and at boundaries will not be a simple 2-dimensional matter.

*2.1.2. BaF<sub>2</sub> on RABiTS* Goyal et al. [21] carried out EBSD measurements on a YBa<sub>2</sub>Cu<sub>3</sub>O<sub>7-δ</sub> film grown on a RABiTS template by the BaF<sub>2</sub> method. The grain structure in the YBa<sub>2</sub>Cu<sub>3</sub>O<sub>7-δ</sub> layer was found to be of a similar form to that of the substrate, both in terms of grain shape and size and also the degree of crystallographic orientation. Holesinger *et al.*[38] found that in thick YBa<sub>2</sub>Cu<sub>3</sub>O<sub>7-δ</sub> films fabricated by this method, the grain structure does not simply replicate that of the substrate but is inhomogeneous through the thickness. At the top surface there are mesa-like grains around 0.25 μm across, which are part of an upper section with a relatively low density. This can be clearly distinguished from the lower part of the film which has less porosity. The bottom layer has large YBa<sub>2</sub>Cu<sub>3</sub>O<sub>7-δ</sub> grains containing numerous Y<sub>2</sub>O<sub>3</sub> precipitates and a small number of planar defects whilst the upper half of the film with smaller YBa<sub>2</sub>Cu<sub>3</sub>O<sub>7-δ</sub> grains has fewer precipitates, more planar defects and a significant number of secondary oxide and oxy-fluoride phases. There is a distinctive layer consisting of Ba, O and F which separates the two parts of the bimodal structure. In addition, cross sectional TEM in this work demonstrated significant meandering of boundaries, suggesting a laminar rather than columnar growth mechanism.

Feldmann *et al.*[28] investigated such samples further using EBSD mapping and showed that the nature of the grain boundary networks in the lower part of the YBa<sub>2</sub>Cu<sub>3</sub>O<sub>7-δ</sub> film depend on the total film thickness. By progressively thinning a sample, they were able to build up grain boundary maps of a region not only at different thicknesses within the superconductor, but also in the YSZ buffer and underlying NiW substrate. A film which was just 0.5 μm in total thickness was studied at a height of 0.45 μm (after removing 50 nm) and the grain structure was found to replicate that of the YSZ buffer, indicating regular columnar growth of YBa<sub>2</sub>Cu<sub>3</sub>O<sub>7-δ</sub> grains nucleated epitaxially by the substrate. However a 1 μm film showed a very different growth morphology. A significant amount of sideways meandering of the grain boundary was seen, both in the plane of the film and also through the thickness. A grain boundary 800 nm up from the base of a 1 μm-thick film may be displaced laterally by as much as 10 μm from the position of the boundary in the buffer layer. Even thicker (2.5-2.9 μm) films were also studied, and as these have the bimodal structure previously described, EBSD measurements were made 0.2 μm from the base of the film (after ion-milling). A greater degree of meandering was observed in these samples and some boundaries in the YBa<sub>2</sub>Cu<sub>3</sub>O<sub>7-δ</sub> layer were observed to be completely uncorrelated with boundaries in the buffer layer. The significance of this meandering both in the plane as well as through the thickness is that grain boundaries will have a significantly greater cross-sectional area than planar ones.[15, 39]

*2.1.3. MOD on RABiTS* Due to the desire to produce a thick film over a large area in a short time in order to minimise total cost, several more-scaleable methods have become popular for the deposition of the superconducting layer. One such technique is metal-organic deposition (MOD), utilised by American Superconductor Corporation. Progress using this technique has been rapid and high values of  $J_c$  can be achieved in thick films[40, 22], despite such films including a number of second phases and porosity. A comprehensive discussion of the progress and challenges involved in optimising such chemical solution deposited coated conductors is found in Holesinger *et al.* [41]. As with the BaF<sub>2</sub> method, MOD-processed films

have been noted to have a distinct layered rather than columnar microstructure[42]. Plan-view SEM of films milled to varying thicknesses show significant porosity (though with the amount of porosity decreasing towards the base of the film) and TEM cross sections highlight the laminar, porous microstructure[44].

The nature of the grain boundary networks in 0.8  $\mu\text{m}$ -thick MOD films has been investigated[27]. EBSD measurements showed definite positional correlation between buffer layer grains and  $\text{YBa}_2\text{Cu}_3\text{O}_{7-\delta}$  grains, along with a significant improvement in the texture of grains, especially the out-of-plane alignment. The improvement in out-of-plane alignment of  $\text{YBa}_2\text{Cu}_3\text{O}_{7-\delta}$  grains was not uniform or random, but was found to be greatest above the template grains with the largest out-of-plane misorientations. A sub-grain structure was visible, particularly above template grains with largest out-of-plane misalignments. TEM measurements also indicated multiple grains above template grains and reveal a significant degree of meandering through the thickness.

The mosaic of  $\text{YBa}_2\text{Cu}_3\text{O}_{7-\delta}$  sub-grain orientations in films produced by this process has recently been studied in detail using microdiffraction techniques[45]. This indicated that the  $\text{YBa}_2\text{Cu}_3\text{O}_{7-\delta}$  mosaic spread above a single Ni grain is as low as  $0.7^\circ$  if that Ni grain is well oriented ( $c$  perpendicular to surface), though the mosaic spread increases above the more tilted grains. An interesting finding is that there seems to be some correlation between grain size and the mosaic spread, with large Ni grains leading to a smaller range of orientations in the overlying  $\text{YBa}_2\text{Cu}_3\text{O}_{7-\delta}$ .

The grain boundary networks produced on RABiTS by other chemical routes such as Liquid Phase Epitaxy (LPE)[46] and other fluorine-free methods[47, 48] are yet to be studied in great detail, though it is expected that due to the existence of a liquid phase during superconductor growth, they will exhibit a lateral growth mechanism leading to significant overgrowth of grains.

## 2.2. Growth Texturing

**2.2.1. Grain boundaries in substrates and buffer layers** The IBAD technique generates a preferred texture in the buffer layer, hence it does not require a textured substrate and polycrystalline Hastelloy is often used. An example IBAD structure is shown in figure 1. The primary requirement of the substrate in allowing overgrowth of a well-aligned IBAD layer is that it should have a smooth surface. Early research in this area focused on YSZ[9, 49], but it was determined that a well-oriented film of MgO can be produced in a much shorter time [50]. Iijima and co-workers have also extensively investigated the use of GdZrO layers [11]. Additional buffer layers are required, but the important focus is on the IBAD MgO layer as it is responsible for inducing the alignment in the subsequent layers. The IBAD technique involves producing a texture by bombarding the film with ions as it grows [51]. Typically an appropriate texture can be achieved for a very thin layer ( $\sim 10$  nm),[10, 52] though a homoepitaxial layer may be added before an additional buffer such as  $\text{LaMnO}_3$  is added [13]. However it has been recently shown that even without a homoepitaxial MgO layer, an excellent texture in the  $\text{LaMnO}_3$  layer can be obtained - (002) rocking curves have FWHM values of around  $2.5^\circ$  and (111) phi scans FWHM of around  $6^\circ$  [53]. TEM and EBSD measurements of IBAD-based tapes demonstrate that the grain size achieved within the buffer layers is typically around 100-200 nm, much smaller than that achieved by the RABiTS route [27, 54]. This is of crucial importance in determining the nature of the grain boundary network in the subsequent  $\text{YBa}_2\text{Cu}_3\text{O}_{7-\delta}$  film.

There is an alternative route to production of oriented buffered tapes via the growth process, known as Inclined Substrate Deposition (ISD). This does not involve an assisting

ion-beam but instead has the template layer (usually MgO) depositing with an inclination to the substrate normal. This results in the growth of grains for which the normal to the (002) planes is aligned at some angle intermediate between the substrate normal and the direction of depositing flux. The columnar grains produced by this method have a diameter of around 100 nm and in that sense they are similar to an IBAD template. However there are a number of important differences. The first is that the ISD surface is much rougher, having a corrugated nature. Secondly the average global texture is different from both RABiTS and IBAD templates, being tilted away from the cube texture. Finally the extent of alignment is, at least as developed to-date, not quite as good as for the other methods, with in-plane (002) phi-scans of MgO having a FWHM of around  $10^\circ$  [55, 56, 27, 54, 57, 58].

**2.2.2. PLD on IBAD** As previously detailed in section 2.1.1, deposition by PLD tends to result in a columnar structure with the 2-D grain structure in the  $\text{YBa}_2\text{Cu}_3\text{O}_{7-\delta}$  film closely reproducing that of the underlying layer. On IBAD substrates it has been observed that the spatial locations of some grain boundaries are seen to match up in each layer [59]. However it has been found that the  $\text{YBa}_2\text{Cu}_3\text{O}_{7-\delta}$  grains can be as large as 250 nm across, which is much larger than that of the IBAD grains, suggesting that  $\text{YBa}_2\text{Cu}_3\text{O}_{7-\delta}$  nucleates only on a subset of the IBAD grains [60]. The situation may be complicated by non-uniformities through the thickness of the  $\text{YBa}_2\text{Cu}_3\text{O}_{7-\delta}$  [61] which may be due to reaction of the lower part of the  $\text{YBa}_2\text{Cu}_3\text{O}_{7-\delta}$  with the buffer layers.

**2.2.3.  $\text{BaF}_2$  on IBAD** There has been detailed study of the ex-situ  $\text{BaF}_2$  process on IBAD substrates. This method produces very different grain boundary networks from  $\text{YBa}_2\text{Cu}_3\text{O}_{7-\delta}$  films grown by PLD, due to extensive lateral overgrowth of grains, as demonstrated by TEM[38]. Grains observed near the base of thick films are as much as 50 microns in diameter, despite growing on IBAD substrate grains as small as 100-250 nm. This lateral grain size is more than 17 times wider than the film thickness and so it is thought that this lateral growth is mediated by the presence of a liquid phase during processing. In fact the situation is rather complex as the extent of lateral overgrowth depends on  $\text{YBa}_2\text{Cu}_3\text{O}_{7-\delta}$  film thickness. Thick  $\text{BaF}_2$ -processed films have been known for some time to have a bimodal structure[62], as discussed for growth on RABiTS substrates and has been shown to have lateral layers separated by  $\text{Ba}_2\text{Cu}_3\text{O}_y$  layers. More recent EBSD measurements comparing the structures 900 nm from the base of films grown to different thicknesses had very different microstructures. Whilst large grains ( $50 \mu\text{m}$  plus) develop in the lower section of thick ( $2.9 \mu\text{m}$ ) films, a film which is grown only  $1.1 \mu\text{m}$  thick developed grains only a few microns in diameter near the base [106]. The fact that this is still significantly larger than the substrate grain size indicates that the same overgrowth process occurs but does not cause the same extent of lateral grain growth. Magneto-optical measurements have also been made on these samples which demonstrate that the electromagnetic properties are consistent with what would be expected from the observed (2-dimensional) grain structure in the superconductor.

**2.2.4. Chemical growth methods on IBAD substrates** Another important process is the use of metal organic chemical vapour deposition (MOCVD) which has most widely been carried out on IBAD substrates. Films grown by MOCVD have been observed to be dense and uniform [63] though with a "dead layer" near the surface which does not carry a significant amount of current [64]. Little further investigation of grain networks in MOCVD films has been carried out to date. Superconducting layers have been grown on IBAD conductors using a similar MOD process to that described previously for RABiTS. For example Kitoh et al.

have described the growth of Sm doped YBCO on IBAD-GZO buffer layers. No detailed description of the resulting grain properties has yet been published, however.

### 3. Single Grain Boundaries

In this section we review the observed behaviour of single grain boundaries in  $\text{YBa}_2\text{Cu}_3\text{O}_{7-\delta}$  with an emphasis on those with misorientation angles less than 10 degrees. This cutoff is chosen following the work of Redwing and Heinig [65, 7] who showed, with some variation with magnetic field, that boundaries with larger angles are Josephson junctions whilst those with small misorientation angles are strongly coupled. As discussed previously, it is only these low-angle grain boundaries (LAGB) which are relevant in modern coated conductors. The defining property of a low-angle grain boundary is that it consists of a series of dislocation cores with a strained lattice in-between, rather than a continuous non-superconducting layer. At the transition between the low-angle and high-angle regimes, the grain boundary energy ceases to increase linearly with grain boundary angle, as there is significant overlap of the strain fields.

#### 3.1. Dependence of Critical Current on Grain Boundary Misorientation Angle

The earliest work on the properties of grain boundaries in high-temperature superconductors is that of Chaudhari and Dimos, soon after the discovery of  $\text{YBa}_2\text{Cu}_3\text{O}_{7-\delta}$  [66, 67, 5]. Their work involved the isolation of current tracks crossing a grain boundary in a film grown on a bi-crystal substrate. In this way a defined single grain boundary could be isolated for direct electrical measurement of its critical current density. This technique, producing a lithographically-patterned, boundary-crossing current track on a bi-crystal substrate, has been used in the majority of other studies of the electrical transport properties of grain boundaries. Until recently, when it became possible to extract single grain boundaries from coated conductors this constituted the only way of accessing the properties of  $\text{YBa}_2\text{Cu}_3\text{O}_{7-\delta}$  grain boundaries in isolation (with the notable exception of 45 degree misorientations created by the bi-epitaxial method due to Di Chiara et al [68], these are however high-angle boundaries and not relevant to this article).

The first published plot of the variation of critical current with grain boundary angle  $\theta_{\text{gb}}$ , due to Dimos [5], showed an exponential decrease of critical current with increasing angle (although at the time interpreted as a  $1/\theta$  dependence), figure 2a shows an updated version of Dimos' plot containing data sourced from a number of authors. Figure 2 shows the single data set obtained by Verebelyi et al. [69] including bi-crystal boundaries, IBAD and RABiTS boundaries. The exponential dependence is well established, although at various times some authors have postulated the existence of a "low-angle" plateau. In particular Heinig et al. [65] postulated that grain boundaries as large as  $7^\circ$  do not affect the transport current. Set against this are studies such as that by Verebelyi showing a dependence down to  $3\text{-}4^\circ$  [69], although below  $3^\circ$  the deleterious effect is noted to be quite limited at 77 K [70]. More recently Horide et al [71] in one experimental series distinguishes between the "plateau" ( $\theta_{\text{gb}} < 2^\circ$ ), LAGB ( $2^\circ < \theta_{\text{gb}} < 10^\circ$ ) and Josephson junction  $10^\circ < \theta_{\text{gb}}$  behaviour regimes. Where plateaus extending beyond  $\sim 2^\circ$  are found it is possible that this simply reflects poor intra-grain critical current. However, Verebelyi [70] noted that a  $2^\circ$  grain boundary has the same effect on the critical current as the twin boundaries that are unavoidable within the grains in a practical superconducting layer.

While the overall behaviour of the critical current follows an exponential decrease it is apparent that there is a cross over in mechanism. Consequently it is likely that the exact form

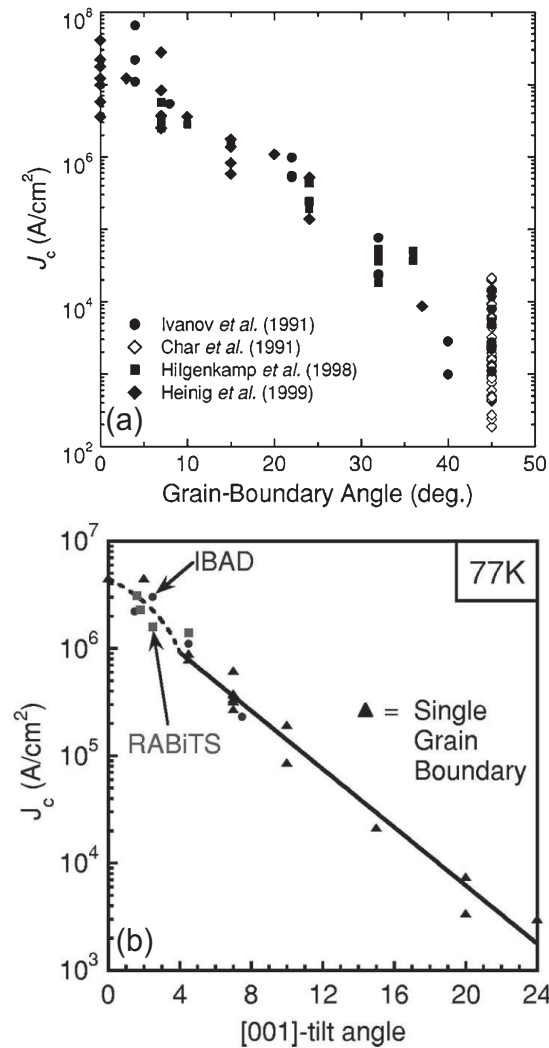


**Figure 2.** Critical current density of [001]-tilt grain boundaries with varying misorientation angles from a number of authors. Figure (a) is reproduced from [6] with permission. Figure (b) is reproduced from [69] and shows a the reduced scatter found with a single data set. Also shown on the same plot are a RABiTS and an IBAD grain boundary. In plot (b) it is possible to observe indications that the dependence of critical current with grain boundary misorientation angle is different between the HAGB and LAGB regimes.

of the  $J_c(\theta_{gb})$  plot is not the same below and above the cross over [65, 7]. Although the data admits of range of fits there are indications of this in the work of Verebelyi et al. as shown in figure 2b.

If the critical current at the grain boundary is lower than that found in the grains, it follows that the available pinning force, even in self field, is suppressed. That the vortex pinning force density at low-angle grain boundaries is lower is supported by studies of the form of the current-voltage ( $I$ - $V$ ) curves seen at single grain boundaries. These are found to be sharper than those found in grains. This is explained in terms of the whole electric field being generated across the grain boundary leading to straightforward viscous flux flow rather

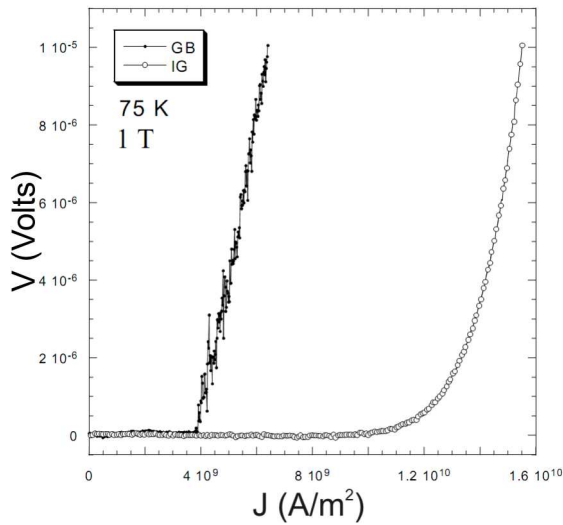


**Figure 3.** V-J curves for LAGB and IG material at 75 K and 1 T applied field parallel to the c-axis for a  $3.8^\circ$  boundary. The different nature of the two transitions is readily apparent. This figure is reproduced from [124] with permission.

than the flux creep more commonly seen in  $\text{YBa}_2\text{Cu}_3\text{O}_{7-\delta}$  grains and single crystals. Grain boundary  $I$ - $V$  curves, an example of which is shown in figure 3, thus show a more well-defined transition than those for in grain tracks [72, 73, 74, 124]. That the grain boundary forms a weak-pinning plane is a recurring observation in the in-field measurements discussed in the following section.

Whilst the work described so far considered mainly the effects of in-plane [001] tilt boundaries, the general situation will be more complex with an arbitrary grain boundary being able to have any combination of the misorientation types shown in figure 4. In the thin film model system it is relatively easy to generate a [001] boundary but the other two have not been extensively studied. Nonetheless in coated conductors it is perfectly possible to see as much misorientation about the other two axes as about the [001] axis, this represents one of the significant differences between model system boundaries and those found in coated conductors. Goetz, as reported in [6], showed that the critical currents of [001] and [100] tilt boundaries were comparable, [100] twist boundaries had a more significant deleterious effect on the critical current of up to an extra order of magnitude reduction in  $J_C$ .

### 3.2. The In-Field Properties of Grain Boundaries

Magnetisation methods, as opposed to direct transport measurements, are easier to perform but are not particularly suitable for studying single grain boundaries, since the current can simply circulate within the grains. Magnetisation measurements have been developed to study separately IG and GB properties in coated conductors [75, 76] but this method does not give satisfactory results with single boundaries. However, by lithographically patterning a current ring both Verebelyi [70] and Thompson [77] have directly measured the critical current properties of double grain boundaries. Here the patterned track forces the induced

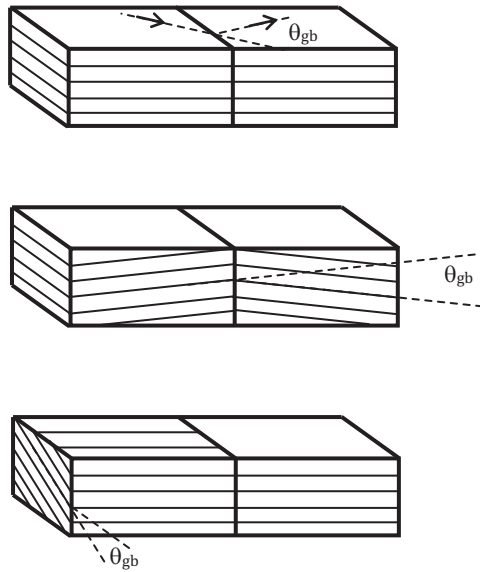


**Figure 4.** These schematics show, from top to bottom, orientation of a [001] tilt boundary, a [100] tilt boundary and a [100] twist boundary in a cubic bi-crystal.

current to cross the grain boundary in two defined places.

Although intrinsically limited to low-field regimes several authors have reported Magneto-Optical measurements of the penetration of vortices at grain boundaries. When studied in increasing field from the virgin state it is seen that magnetic flux first penetrates at the grain boundary showing that the vortex pinning is weakest at the grain boundary. The first such results were reported by Polyanskii et al [78]. The MO technique is however limited by the field range of the indicator film employed. Equally, scanning hall microscopy measurements by Perkins [79] show similar preferential flux flow along grain boundaries as shown in Fig. 5.

One important field dependent effect seen in transport measurements on grain boundaries is that at a cross over field (typically  $> 2$  T) the IG properties are recovered [30, 78, 69]. Consequently in such high fields it is the properties of the grains, including any pinning enhancement present [80], that are observed. This is essentially due to the weakly pinned vortices at the boundary interacting with the strongly pinned vortices in the grain [81]. In simple terms this arises because if the vortex-vortex distances are small, as at high field, the well pinned IG vortices can inhibit the motion of the weakly pinned GB vortices along the grain boundary. Such an IG to GB behaviour cross-over with field has been reported widely for the complex multiple grain boundary systems found in coated conductors and this is discussed in the next section. In addition to absolute measurements of the critical current, the dependence on field-magnitude and field-orientation of such boundaries has been studied. Diaz *et al.* [82] showed that for a field rotated within the grain boundary, enhanced pinning was seen at a particular angle which was associated with pinning along the vortex cores. It should be noted here that the enhanced pinning was found whilst rotating the field within the grain boundary, the dislocation cores did not raise the observed critical current to the

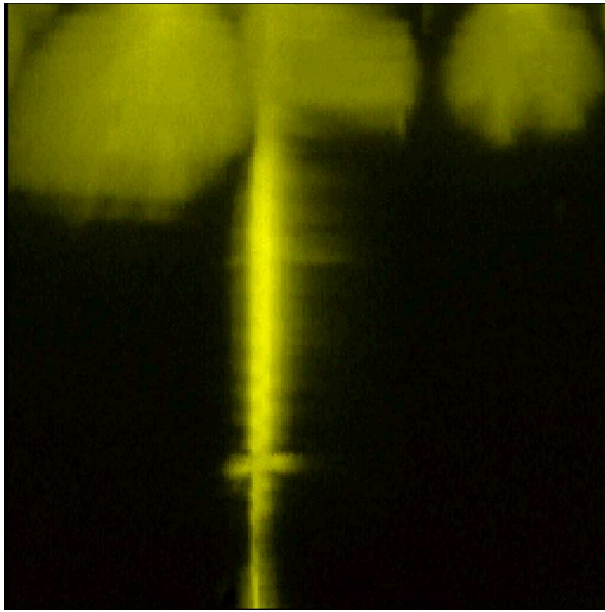


**Figure 5.** Preferential penetration of flux along a [001]-tilt grain boundary in  $\text{YBa}_2\text{Cu}_3\text{O}_{7-\delta}$  at 77 K imaged using a scanning hall probe [79]. The sample has been cooled in zero field and the applied field then ramped up to 18 mT. Yellow indicates flux penetration although the colour scale is arbitrary. Image courtesy G. Perkins.

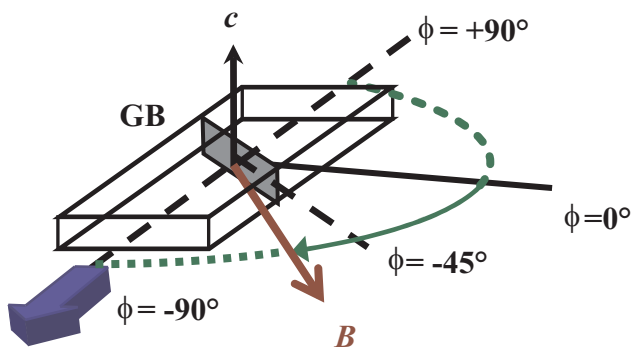


**Figure 6.** Geometry of a measurement of the effect of in-plane field rotation on the critical current of a bi-crystal boundary. Here the boundary is at an angle to the current direction in order to reduce the symmetry of the measurement.

level of the grains. Hogg *et al.* [74] found that the reverse field through the grain boundary from vortices trapped in the grain can give rise to angular hysteresis effects, similar to critical current versus field hysteresis effects seen in  $\text{YBa}_2\text{Cu}_3\text{O}_{7-\delta}$  powder-in-tube conductors [83] and recently in coated conductors [84].

Durrell *et al.* [85] demonstrated that vortex channelling at grain boundaries can depend on the field orientation, and that for certain orientations of field low-angle boundaries do not reduce the observed critical current. Most in-field measurements are performed with the

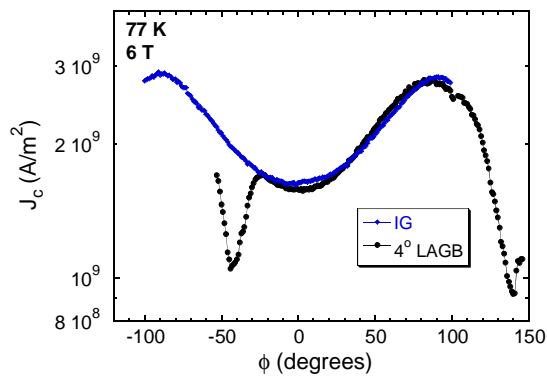


**Figure 7.** Comparison of the variation of critical current with rotation of in plane field for a track crossing a  $4^\circ$  bi-crystal boundary. Only when the applied field is near parallel to the grain boundary is the critical current affected by the presence of the grain boundary.

field oriented along the  $c$ -axis, so it is generally always the case that there is a component of the Lorentz force pointing along the weak pinning channel. In measurements performed with in-plane fields as shown in figure 6, except for the particular orientation of field parallel to the grain boundary, most of the flux vortex is strongly pinned. As might be expected in these geometries the critical current of the grain boundary is either not suppressed at all, or much less suppressed as compared to the field parallel to grain boundary configuration. This observation may explain why low-angle grain boundaries do not seem to significantly reduce the critical current in measurements where the field direction is not well controlled, such as in magnetisation measurements. An example of the data recorded in such a measurement is shown in figure 7. It should be noted that the critical current of the IG and GB tracks compared are almost identical except when the applied field is near parallel to the boundary.

Horide et al. [86] have recently presented evidence of a similar angular dependent crossover from IG to GB limited critical currents for out-of-plane field angle tilts. Interestingly the effect they observe is only apparent at high fields, which are normally associated with GB behaviour for all applied field angles.

### 3.3. Theory of Critical Currents at Grain Boundaries

Having reviewed what measurements on thin film bi-crystals actually tell us about grain boundary properties a brief examination of the underlying theory is warranted. It is apposite in this discussion to remember that critical current is always controlled by the strength of vortex pinning in the available cross section of conductor, in these low-angle grain boundaries Josephson coupling effects do not apply.

The simplest model for the current transport at a grain boundary is that put forward by Chisholm and Pennycook [87] who considered that the currents flow in the regions between the dislocation cores at the grain boundaries. If the effect of the strain field around the dislocation cores is considered it is possible to arrive at a simple model which describes how the critical current falls as the available area for current flow decreases. From their criterion of a 1% strain leading to suppression of superconductivity they suggested that for a  $5^\circ$  misorientation the effective size of the dislocation cores is 2.9 nm along the boundary and 8.9 nm perpendicular to it. While this model indeed predicts some of the properties of the grain boundary it cannot explain the angular dependent channelling effect or the fact that at

high field  $J_{c,gb}=J_{c,ig}$ .

Gurevich [81] has postulated that this is due to the vortices at the grain boundaries having an enlarged core in which the order parameter is not fully suppressed. This arises from the effect of the dislocation core generated strain fields on the electronic properties of the grain boundary. These distinct Abrikosov-Josephson (A-J) vortices are intrinsically more weakly pinned since the change in the free energy of the system arising from placing such a vortex on a pinning site is smaller. This concept neatly explains the experimental evidence which all indicate that there is vortex channelling at the grain boundary, suggestive of a weak pinning plane. The Gurevich model also describes the LAGB to HAGB cross over in terms of the conversion of A-J vortices into fully developed Josephson vortices. Although Gurevich's work is comprehensive and detailed the critical conclusion for most that the reduction in the critical current at LAGB is due to reasons significantly more subtle than simple reduced cross sectional area. As suggested by the work of Durrell et al. [85] if ways can be found to enhance the pinning on A-J vortices, which may be simply geometrical, the critical current of the grain boundary can be increased. This is a fundamentally different approach to attempting to change the electronic structure of the grain boundary through Ca doping.

### 3.4. Single Grain Boundaries Isolated Within Coated Conductors

The preceding discussion has concerned the properties of what are sometimes termed "artificial" grain boundaries in thin films grown on bi-crystal substrates. These are contrasted with the "natural" grain boundaries found in coated conductors. Feldmann et al. [15] isolated such grain boundaries with a range of misorientation angles in  $YBa_2Cu_3O_{7-\delta}$  films grown on by both MOD and PLD on RABiTS conductors. As described earlier, they found that the straight grain boundaries grown by PLD are somewhat similar to those found in bi-crystal structures. Indeed MO characterisation of such samples again indicates that the GB are weak pinning channels [88]. The situation with films grown by the MOD process is considerably more complex. Feldmann found that as such grain boundaries are highly meandered, they can support a higher critical current density than those found in PLD/RABiTS. An example of such a boundary is depicted in figure 8. This is associated both with the increased cross sectional area of these meandered boundaries and the suppression of the vortex channelling, it is impossible for a vortex to lie wholly within a meandered boundary meaning some sections are more strongly pinned, increasing the observed critical current. As an alternative to meandered grain boundaries, the use of grains with large aspect ratios was proposed as a potential route to enhance the cross sectional area of the grain boundary [89, 90, 91]. That such grains do provide enhanced properties has been demonstrated by Eickemeyer *et al.* [16]. Interestingly it should be noted that bi-crystal boundaries do meander on length scales of a few hundred nm [92, 93, 39]. Gray et al. [94] noted that atomically flat bulk bi-crystal boundaries exhibit a depressed critical current when compared to equivalent misorientation angles in meandered boundaries in thin film bi-crystals. In a similar manner as to the proposed mechanism for the enhancement of MOD GBs over PLD GBs, the difference between bulk and thin film grain boundaries may well be due to the partial suppression of easy vortex motion at the boundary as the vortex cannot lie entirely within the weakly pinned boundary [95].

### 3.5. LAGB grain boundaries are weak pinning planes

Single low-angle boundaries demonstrate a roughly exponential dependence of critical current on misorientation angle which persists down to small ( $\sim 2^\circ$ ) misorientations. Although

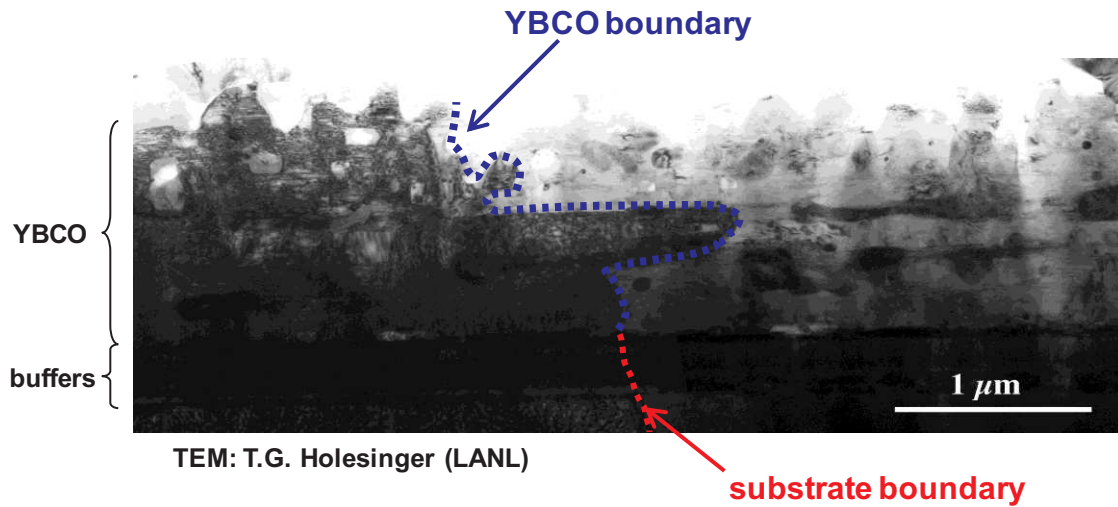


**Figure 8.** A micrograph of a meandered grain boundary in a RABiTS conductor. The highly convoluted nature of the grain boundary is clearly evident. The position of the grain boundary on the surface on the conductor can be some distance from the substrate grain boundary. Micrograph from [28] courtesy T. G. Holesinger.

the coupling across the grain boundary is strong, in that the order parameter is continuous and there is no Josephson junction, the pinning at the grain boundary is weaker than in the grain. Simply put then, this is the cause of the reduced critical current seen in low-angle grain boundaries.

The fact that the low-angle grain boundary constitutes a plane of weak pinning means that for fields directed along the  $c$ -axis the critical current is always reduced over the in-grain value, unless the applied field is large enough that IG vortices serve to pin GB vortices. For other field orientations where individual vortices lie both in-grain and across the grain boundary, or for the case of meandered boundaries where the vortex cannot align entirely with the boundary, it is possible for the strong pinning of the segments of vortex in the grains to prevent the motion of the weakly pinning vortex segments enhancing  $J_C$ .

#### 4. Effect of Grain Boundaries on the Critical Current Properties of Coated Conductors.

Having reviewed the properties of single low-angle grain boundaries in  $\text{YBa}_2\text{Cu}_3\text{O}_{7-\delta}$  we proceed to reviewing how transport measurements on coated conductors reflect the nature of the underlying arrangement of grains and grain boundaries. These may be accessed through conventional measurements of transport critical current and through measurements of magnetisation properties. It is also possible to extract information by studying fields which are rotated with respect to the  $c$ -axis direction, rather than simply looking at the case where field is applied along the  $c$ -axis. Finally there are certain materials where it is difficult to see effects to due grain boundaries, whether this be due to very good grain to grain alignment or to the meandered grain boundaries is discussed in the last section.

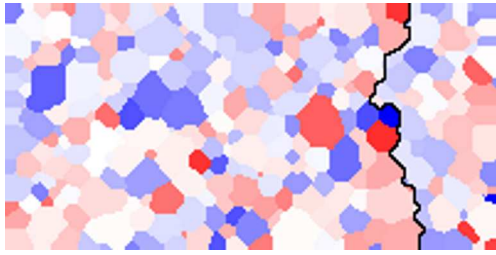


**Figure 9.** Schematic of a coated conductor with various grain alignments showing a possible limiting path perpendicular to the current flow direction.

#### 4.1. Transport Measurements

As transport measurements of coated conductors directly probe the primary characteristic of merit for a coated conductor, they are a good starting point when considering the importance of low-angle grain boundaries. Simple consideration of the force balance equation leads to the conclusion that in a homogeneous superconducting track the critical current is reached in all parts of the track at the same current and the vortices start moving simultaneously. However, as has been demonstrated by imaging the current paths using scanning laser imaging of dissipation [96, 32], in a coated conductor there will be one initial channel cutting across a current path at which flux motion first occurs. This path, in which flux motion starts, represents the lowest critical current in the sample and must stretch from edge to edge. As the current is further increased further additional flux flow regions will appear giving a gradual  $I$ - $V$  transition. The way in which the individual  $I$ - $V$  curves of parts of the sample combine has been discussed by several authors [73, 97]. Essentially in a multiple grain superconductor the overall  $I$ - $V$  curve can show a fairly gradual transition even if the transitions of the individual parts are sharp. The steepness of the overall  $I$ - $V$  criteria is an important factor in magnet design, a material with a very sharp transition needs to be operated some distance from the transition to avoid the sudden generation of heat and destruction of the conductor. Consequently while the shape of  $I$ - $V$  characteristics are a useful way of distinguishing between grain critical current properties and grain boundary properties, in a coated conductor where the current carrying properties of both grains and grain boundaries vary it is a significantly less useful measurement.

**4.1.1.  $J_C(B)$  characterisation** In transport measurements it is, nonetheless, possible to discern GB and IG dominated regimes fairly straightforwardly. The primary source of information is the form of the  $J_C(B)$  dependence. This is seen to change with increasing field [30] and is attributed to the weaker variation of critical current with applied field seen at grain boundaries. Consistent with observations of the behaviour of individual grain boundaries in-grain critical current behaviour is seen at high temperatures and fields whilst grain boundary behaviour dominates at lower temperatures and fields. At 77 K the cross over between IG and GB behaviour was found to be, in the PLD grown layers on RABiTS studied, about 4 T. Below 60 K the transition was already apparently above 9 T. At relatively low fields hysteresis effects in  $J_C(B)$  are observed due to return field from flux trapped in the grains passing through the grain boundaries [84].

As is discussed in detail in the next section, there is an interrelation between the number of grains across the width of a conductor and the ease of current percolation. If percolation is primarily required to evade grain boundaries with poor critical currents it might be expected

that a dependence of critical current on track width should be observed in the GB dominated regime, yet not at high field where the grain boundaries no longer limit critical current. This is indeed observed by Kim *et al.* [98] in MOD grown  $\text{YBa}_2\text{Cu}_3\text{O}_{7-\delta}$  films on a RABiTS substrate. In this material they found the width dependence disappeared at 1 T at 85 K, 2.5 T at 77 K and 4 T at 50 K. In contrast to the results of Fernandez *et al.* [30] there was evidence that the critical current was controlled by grain properties even at 50 K in a field lower than the cross-over field identified by Fernandez *et al.* at 77 K. This may well be due to the meandered grain boundaries found in such MOD conductors, this is discussed in more detail later in this section. The authors also note that they found some sections of their conductor where no clear width dependence of the critical current was observed, again potentially due to the much improved current carrying capacity of meandered grain boundaries.

*4.1.2. Field angle characterisation* Interestingly there is little reported work on determining the contribution to the critical current of grain boundary effects on  $\text{YBa}_2\text{Cu}_3\text{O}_{7-\delta}$  films grown on IBAD conductors. This may well be due to the better grain to grain alignment and smaller grains found in IBAD type conductors meaning that grain boundaries never significantly control the observed critical current [99]. Rutter *et al.* [100] have used characterisation of the in-plane dependence of the critical current in coated conductors where the substrate system is RABiTS and IBAD to argue that the grain boundary network leads to percolation and thus local current flows which are not aligned with the macroscopic current flow. Conversely in IBAD if grain boundaries are not an impediment to current flow the current should be less percolative. Rutter *et al.* [100], found that the force free effect, where the field and the current align minimising the Lorentz force and thus maximising the critical current, is significantly less prominent in RABiTS type conductors than in  $\text{YBa}_2\text{Cu}_3\text{O}_{7-\delta}$  films grown on single crystal or IBAD substrates. This provides evidence that the supposition that grain boundaries play a larger role in the behaviour of RABiTS conductors than IBAD conductors is valid.

#### 4.2. Magnetisation Measurements

Grain-boundary and in-grain critical currents can be difficult to distinguish in magnetisation measurements, not least because if the volume of superconductor probed is large the recovered value for the critical current is, of necessity, an average. Nonetheless there are two broad classes of techniques employed, as with single grain boundaries. First there are magnetic imaging techniques, which have the advantage of showing the local critical current behaviour [101] and secondly traditional approaches based on the analysis of  $M$  vs  $H$  data [102] where techniques can be used to unpick the grain and grain boundary contributions to the overall signal.

*4.2.1. Magnetic imaging* As has been seen in the previous section the imaging of the vortex flow in a superconductor can provide direct insight into the grain boundary properties, showing immediately if there is preferential vortex penetration along grain boundaries. As with single crystals the two main techniques are scanning hall probe imaging and the use of magneto-optic indicator films [88, 32]. While magneto-optic imaging is restricted by the indicator film to fields of a few hundred millitesla, hall probe imaging can work in relatively high fields of the order of a few tesla. Indeed, a reel to reel scanning hall probe technique is used for the rapid characterisation of coated conductors [103]. As for the case of single grain boundaries, and given that at low fields it is always the grain boundary that limits the critical current, flux tends to first penetrate the coated conductor along the grain boundaries. Figure 10 shows flux penetrating from a cut in a MOD/RABiTS tape in a similar way to that

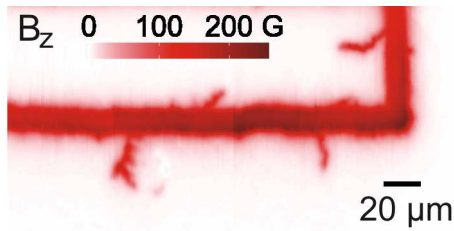


**Figure 10.** A scanning hall probe image of flux penetrating a MOD/RABiTS coated conductor from a cut as in [88]. At these low fields the flux preferentially follows the weak pinning grain boundaries. This image is courtesy R. Dinner.

described in [88]. Magneto-optic imaging was used by van der Laan et al. [104] to map the distribution of grain boundaries in a RABiTS based coated conductor. From the distribution of flux penetration in to the conductor they were able to show that, as has been observed in transport measurements, the current flow in such materials is highly percolative with even defects parallel to the current direction affecting the macroscopic transport current.

*4.2.2. Critical currents from magnetisation measurements* Magnetisation measurements of critical current can give rise to difficult problems of interpretation[102] however they have the advantage that no contacts are required and the technique is non-destructive. Tönies *et al.* [76] established a method for distinguishing between grain boundary and intra-grain contributions to the overall critical current behaviour by looking for a characteristic signature in the second derivative of the  $M-H$  loop. In this way they were able to determine the in-grain and grain boundary critical currents of an  $\text{YBa}_2\text{Cu}_3\text{O}_{7-\delta}$  coated conductor sample. In a series of articles Palau and coworkers have extensively employed a similar technique, based on the identification of a peak in the  $M-H$  loop caused by material granularity, to study the in-grain and grain boundary contributions to the overall behaviour of IBAD and RABiTS based coated conductors[75, 105]. In particular they have used magnetisation measurements to study the effect of the extent to which the superconducting layer adopts the granular structure of the substrate [106]. This technique has also been applied to the interaction between in-grain and grain boundary vortices of ex-situ  $\text{BaF}_2/\text{RABiTS}$  samples of different thicknesses [107] and to study the suitability of using AC susceptibility measurements to study the grain boundary network in coated conductors[108].

### 4.3. Meandered Grain Boundaries

In the previous section we discussed the fact that meandered grain boundaries exhibit superior properties to more planar boundaries. In an important series of papers Feldmann has shown that the grain boundaries in RABiTS with  $\text{YBa}_2\text{Cu}_3\text{O}_{7-\delta}$  layers grown with ex-situ techniques do not fully reproduce the granular structure of the substrate material if the film is sufficiently thick[28], that the grain boundaries exhibit a significant meander and that the boundary at the top of the  $\text{YBa}_2\text{Cu}_3\text{O}_{7-\delta}$  layer can be up to 10 microns from the 'seed' boundary[27, 28]. This results in a significantly higher critical current in coated conductors that contain such meandered grain boundaries due to their larger cross sectional area and the suppression of vortex channelling due to the meander of the boundary [15].

#### 4.4. Outlook

When incorporated into a coated conductor the existence of grain boundaries, and their distinct  $J_c(B)$  and  $J_c(\theta, \phi)$  characteristics tend to result in a very complex critical current landscape. That is to say as one moves across the field, temperature and field orientation parameter space, at any one set of conditions a proportion of the grain boundaries in a coated conductor may constitute locally the limiting factor on critical current performance with the remainder due to in grain properties. This means that trying to decompose the observed critical current behaviour of coated conductors in terms of separate grain and in-grain properties is not simple. What is required is a model into which the various parameters may be input, and this is discussed in the next section.

### 5. Models of Coated Conductors as Networks of Grains and Grain Boundaries

Modelling coated conductors as grain/grain boundary networks is a valuable tool in understanding how tapes can be optimised for the appropriate application. Modelling has helped build an understanding of how the reduction of the deleterious effects of grain boundaries is crucial in diminishing the influence of conductor dimensions (important if conductors are to be subdivided) and grain size. This section explores how models have been developed to describe percolation of current in grain boundary networks, how they have been used to explain the shape of observed  $I$ - $V$  characteristics and the implications that these results have for the ongoing technological development of coated conductors.

#### 5.1. Approaches to Modelling Grain Boundary Networks

An early model of current flow in coated conductors is that of Specht et al. [109] which identifies two possible approaches, considering either the grains or boundaries. A *bond percolation* model identifies each grain boundary as being either "conducting" or "non-conducting" (based on its misorientation angle) and assigns a critical current based upon the cross-section of the tape which remains conducting. An alternative *site percolation* approach assigns each grain as being either accessible or inaccessible to current. Again it is possible to define the tape performance as the remaining section (at its narrowest part) available for current to flow along once a number of grains and associated boundaries cannot be traversed. Even this simple model is effective in illustrating that the effect of clustering of regions which are obstructive to current-flow is very dependent on sample dimensions. The probability of a percolative path existing through a network of grains and boundaries which may be "on" or "off" varies significantly with tape length and width. Rutter et al. [110] showed that a similar illustration of percolation thresholds in real grain structures measured by EBSD could be considered. By this method, one could plot an EBSD map with varying threshold angles and determine how percolation paths open up as a function of this angle. One important observation is the fact that networks which have high degrees of "area percolation" may still have very low values of the limiting cross section. As such, a simplistic binary on/off model of grain boundaries is difficult to translate into quantitative values for critical currents of coated conductor tapes.

Developing a more quantitative, realistic network model requires first some definition of grains in the model (both positionally and orientationally) and subsequently an assignment of the electromagnetic characteristics of the grains and boundaries based on their physical configuration.

### 5.2. Microstructural Models

A crucial assumption which has underpinned models of coated conductors as grains and grain boundaries is that the coated conductor can be described in 2-dimensions. This seems a reasonable approximation given that the superconducting layer is thin and the grain morphology is determined by the underlying substrate. A very simple model of such a 2-D structure is with a lattice of identical polygonal grains, i.e. squares or hexagons [111, 112, 109]. The crucial difference between these from a percolation viewpoint is the number of neighbours each grain has. Analysis of real 2-dimensional grain structures shows that the number of neighbours is usually close to 6 and so the hexagonal structure is probably a more accurate representation. Another option is to use a brick-wall structure, in which grains have 6 neighbours. A development of this structure is to vary the lengths of the "bricks" in order to investigate the possible effect of grains with large aspect ratios. [90, 91]

Whilst these simple model grain structures are straightforward to scale to long lengths, they do not closely resemble real grain networks. Holzapfel and co-workers [30, 113] have therefore applied network models to real grain structures which have been measured by EBSD. One significant advantage of this is the ability to prove the functionality of such a modelling method in describing an area of conductor whose properties can actually be measured [114]. The method is obviously limited to the size of sample which can be measured using EBSD. Rutter & Goyal [115] developed a method of simulating a grain structure with a realistic appearance, having grains with dissimilar shapes and sizes [116]. This simulation can be scaled to many thousands of grains and can therefore be applied to modelling real conductors and is more appropriate than a structure of identical squares or hexagons. As this model develops the grain structure using a Monte-Carlo growth model it can also be applied to aspected grains. There is still one outstanding problem with the grain structures of all these models. Both the EBSD-measured structure and the Monte-Carlo growth simulation are based on an underlying pixelated grid (of either hexagonal or square pixels) and as such all modelled grain boundaries will be faceted as such.

In addition to the spatial configuration of the grain network, the orientation of grains is crucially important. The advantage of the Holzapfel approach in this respect is that the EBSD measurements also define the grain orientations. With other (simulated) structures the grain or grain boundary orientations need to be assigned in some other way. Some early approaches assigned misorientation angles to grain boundaries based on a distribution, though it is clear that this may result in a non-physical situation.[117, 118] If grains A, B and C all share a common triple-point, then the A-B boundary misorientation cannot be greater than the sum of the A-C and B-C misorientations. Hence the simple solution to this issue is to instead assign the orientations to the **grains** before calculating the boundary misorientations on this basis [110]. Such orientational assignment is generally based on a measurement of orientations of real grains, either in a substrate template or the superconducting film. It is possible to use EBSD data though in the small areas over which such measurements are usually made, it may be that statistical variations produce a non-representative result. X-Ray diffraction measurements usually sample many more grains and so should give a representative set of data. An important step is to show that the two alternative methods produce essentially equivalent results. This would not be the case if adjacent grains had orientations correlated with each other and in considering this it is important not to be misled by neighbouring pixels within the same grain (which are of course highly correlated!). Although much modeling has been carried out considering only the effect of in-plane misorientation (which is often reasonable due to the fact that  $\text{YBa}_2\text{Cu}_3\text{O}_{7-\delta}$  often grows with excellent *c*-axis alignment) it is preferable in general to allow grains to have any 3-dimensional orientation in order to have

the possibility of considering the effect of boundaries whose character is other than simple  $c$ -axis tilt.

### 5.3. Calculating the Critical Current

Once the network of grains and boundaries is described in terms of spatial and orientational configurations, models then assign critical current values to the grain boundaries. This could be as simple as assigning a 0 or 1 in a binary method as previously outlined, though more commonly  $j_c$  values have been based on experimental measurements of low-angle bi-crystal grain boundaries as outlined in section 3.1 and shown in figure 2. Most models consider the properties only of the grain boundaries when calculating the limiting properties, though that developed by Rutter [115] has the advantage that it considers the properties of grains as an integral part of the structure which may, under some circumstances, play a part in the limiting behaviour of the conductor. This will become particularly important if the grains are very well oriented with respect to each other, if they are tilted (vicinal) in nature or if one is considering a regime of temperature or magnetic field in which grain boundaries do not dominate.

Once  $j_c$  values have been assigned, the grains and boundaries can then be described by some simple network theory, representing the grains as nodes and the boundaries as arcs. The problem of calculating the largest current which can cross the conductor (the "maximum flow") can be reduced to one of finding the interface which limits such flow (the "minimum cut") [119]. There are a number of algorithms to achieve this [114, 111, 97], and it is possible to make approximations which trade off a rigorously exact solution in order to be able to efficiently solve a network containing millions of nodes and arcs. The maximum-flow/minimum-cut theorem sheds some light upon what happens physically when the critical current of the conductor is exceeded. There will be dissipation at the interface determined as the location of the minimum-cut which corresponds to it becoming a flux-flow channel [97, 120].

### 5.4. Results of Grain Boundary Models

*5.4.1. Predicting critical currents* Holzapfel et al [114] have demonstrated the general validity of the modelling approach. One use of such models has been to predict the scaling behaviour of coated conductors. The commercial development of tapes has led to gradually increasing lengths and it was initially unclear as to how materials could be processed to achieve very long lengths without the grain boundaries preventing significant decreases in the overall critical current. Such models led to an appreciation that it was crucial to have very sharply textured tapes in order to ensure that an area of highly misoriented grains spanning a significant fraction of the width of the tape was unlikely. Indeed the models have shown that both tape length and width must be considered. If there are just a few grains spanning the width of the tape, the critical current may decrease more rapidly with increasing length whereas when there are many grains across the width the tapes can be made very long without a serious effect [116]. Using a general approach based on Weibull statistics, this relationship has been roughly approximated as [115, 112] as:

$$J_c \propto \left( \frac{1}{N_l} \right)^{\frac{1}{N_w}} \quad (1)$$

where  $N_l$  and  $N_w$  represent the number of grains along the length and across the width of the conductor respectively. As it may be necessary to subdivide the conductors to very small widths to achieve low a.c. losses [121] it would seem to be advantageous to have a very small

grain size, indicating that the smaller grain size of IBAD conductors may be of benefit. Whilst some decreases in  $J_C$  have been observed for very narrow tracks in RABiTS conductors[98], the performance has not been reduced in line with early predictions of the grain boundary models. One reason for this is that the crystallographic textures of the conductors which are presently manufactured are very good, due to well oriented substrates and the fact that the  $\text{YBa}_2\text{Cu}_3\text{O}_{7-\delta}$  grows with a very sharp  $c$ -axis alignment. This results in the grain boundaries having very small misorientation angles such that their behaviour is often not significantly inferior to that of the intra-granular regions. Moreover perhaps a more significant reason that boundaries in such tapes can carry much higher current than predicted by these models is the fact that the boundaries in  $\text{YBa}_2\text{Cu}_3\text{O}_{7-\delta}$  fabricated by chemical methods are not simply planar but are highly meandering in 3-dimensions [28], leading to a much larger interfacial area than was originally expected.

*5.4.2. Modelling I-V characteristics* As well as predicting  $J_C$ , several attempts have been made to model the form of the  $I$ - $V$  characteristic once the critical current is exceeded. Evetts et al. [73] illustrated the importance of the number of active flux-flow channels and showed, based on a triangular distribution of grain boundary misorientation angles, that linear  $I$ - $V$  characteristics for individual boundary segments should lead to a curved characteristic for the overall conductor. Rutter *et al.* [97] then considered the possibility that changes in slope of a tape's  $I$ - $V$  characteristic might be observable. These changes of slope are predicted when the primary flux flow channel branches and upon the formation of further independent channels. Such changes in slope are predicted to be very small in real conductors and so would be difficult to observe. The most detailed model of the  $I$ - $V$  characteristic is that of Zeimetz who used a resistor network model to predict the flux flow channels in grain structures measured by EBSD [122, 120]. Locating the flux-flow channels through such a resistor model was shown [113] to produce similar though not identical results to the maximum-flow/minimum-cut approach. A novel approach to the problem is that of Kiss [123] which addresses flux percolation directly (rather than current percolation) based on a simple cluster model.

### *5.5. Further Requirements of Models*

*5.5.1. Grain boundary morphology in real conductors* Whilst the representations of grains and boundaries in coated conductors has improved from squares and hexagons to something more realistic, the growth modes of real  $\text{YBa}_2\text{Cu}_3\text{O}_{7-\delta}$  films, by chemical methods, do not result in simple 2-D columnar grains. An appreciation of this increased grain boundary interface area is required in future modelling in addition to the implications of current percolation in a third dimension.

*5.5.2. Vicinality of grains* The importance of the properties of the grains themselves must be emphasised in developing models of current percolation in coated conductors. It has become clear that current flow is not exclusively determined by the grain boundaries. One particularly important scenario where the properties of the grains should be considered is for conductors which have inclined grains (i.e. those fabricated by ISD). In this case it is assumed that percolation of current perpendicular to the macroscopic transport direction will be very difficult, based on measurements of films grown on vicinal substrates [125, 126, 127].

*5.5.3. Effect of magnetic field* A factor which has barely been considered in the development of coated conductor models, but is of crucial importance, is the effect of magnetic field. For

fields applied within the plane of the tape, only when the field is aligned with a grain boundary is it expected to have much of an effect on reducing the critical current. Hence development of a model which incorporates the effect of field magnitude and angle is desirable though the appreciation of the non-planar nature of the boundaries makes this a non-trivial challenge.

## 6. Summary

A coated conductor is correctly seen as an assembly of intra-granular and grain boundary elements. The nature of these elements on a microstructural level can vary greatly depending on which of a wide range of processing routes are chosen. Furthermore these elements have different [30, 100] and complex [95, 85, 15] dependencies on temperature and also the magnitude and orientation of magnetic field. We can only satisfactorily describe and explain the overall electromagnetic properties of a coated conductor if we understand the Processing - Structure - Properties relationship at a microscopic level and can recognise how the properties of the individual elements combine to determine the performance of macroscopic superconducting tapes developed for large-scale applications. In this context although grain boundaries may not always limit the critical current of a coated conductor, they are still a key feature. Consequently the science which underpins the development of low-angle grain boundaries with improved current-carrying capacity remains at the heart of future developments in coated conductors.

## References

- [1] D. Larbalestier, A. Gurevich, D. M. Feldmann, and A. Polyanskii. High Tc superconducting materials for electric power applications. *Nature*, 414 (6861):368–377, 2001.
- [2] S. R. Foltyn, L. Civale, J. L. Macmanus-Driscoll, Q. X. Jia, B. Maiorov, H. Wang, and M. Maley. Materials science challenges for high-temperature superconducting wire. *Nature Materials*, 6 (9):631–642, 2007.
- [3] R. E. Somekh, M. G. Blamire, Z. H. Barber, K. Butler, J. H. James, G. W. Morris, E. J. Tomlinson, A. P. Schwarzenberger, W. M. Stobbs, and J. E. Evetts. High superconducting transition-temperatures in sputter-deposited  $\text{YBa}_2\text{Cu}_3\text{O}_7$  thin-films. *Nature*, 326(6116):857–859, 1987.
- [4] D. Dimos, P. Chaudhari, and J. Mannhart. Superconducting transport-properties of grain-boundaries in  $\text{YBa}_2\text{Cu}_3\text{O}_7$  bicrystals. *Physical Review B*, 41(7):4038–4049, 1990.
- [5] D. Dimos, P. Chaudhari, J. Mannhart, and F.K. LeGoues. Orientation dependence of grain-boundary critical in  $\text{YBa}_2\text{Cu}_3\text{O}_7$  bicrystals. *Physical Review Letters*, 61(2):219, 1988.
- [6] H. Hilgenkamp and J. Mannhart. Grain boundaries in high Tc superconductors. *Reviews of Modern Physics*, 74(2):485–549, 2002.
- [7] R. D. Redwing, B. M. Hinaus, M. S. Rzchowski, N. F. Heinig, B. A. Davidson, and J. E. Nordman. Observation of strong to josephson-coupled crossover in 10 degrees  $\text{YBa}_2\text{Cu}_3\text{O}_x$  bicrystal junctions. *Applied Physics Letters*, 75(20):3171–3173, 1999.
- [8] G. Hammerl, A. Schmehl, R. R. Schulz, B. Goetz, H. Bielefeldt, C. W. Schneider, H. Hilgenkamp, and J. Mannhart. Enhanced supercurrent density in polycrystalline  $\text{YBa}_2\text{Cu}_3\text{O}_7$  at 77 K from calcium doping of grain boundaries. *Nature*, 407(6801):162–164, 2000.
- [9] Y. Iijima, N. Tanabe, O. Kohno, and Y. Ikeno. Inplane aligned  $\text{YBa}_2\text{Cu}_3\text{O}_7$  thin-films deposited on polycrystalline metallic substrates. *Applied Physics Letters*, 60(6):769–771, 1992.
- [10] P.N. Arendt and S.R. Foltyn. Biaxially textured IBAD-MgO templates for YBCO-coated conductors. *Mrs Bulletin*, 29(8):543–550, 2004.
- [11] Y. Iijima, K. Kakimoto, Y. Yamada, T. Izumi, T. Saitoh, and Y. Shiohara. Research and Development of Biaxially Textured IBAD-GZO Templates for Coated Superconductors. *MRS Bulletin*, 29(8):564–571, 2004.
- [12] D. P. Norton, A. Goyal, J. D. Budai, D. K. Christen, D. M. Kroeger, E. D. Specht, Q. He, B. Saffian, M. Paranthaman, C. E. Klabunde, D. F. Lee, B. C. Sales, and F. A. List. Epitaxial  $\text{YBa}_2\text{Cu}_3\text{O}_7$  on biaxially textured nickel (001): An approach to superconducting tapes with high critical current density. *Science*, 274(5288):755–757, 1996.
- [13] V. Selvamanickam, Y. Xie, and J. Reeves. Progress in scale-up of 2g conductor at superpower, superconductivity for electric systems 2007 annual peer review, 2007.

- [14] X. Li, M.W. Rupich, T. Kodenkandath, Y. Huang, W. Zhang, E. Siegal, D.T. Verebelyi, U. Schoop, N. Nguyen, C. Thieme, Z. Chen, D.M. Feldman, D.C. Larbalestier, T.G. Holesinger, L. Civale, Q.X. Jia, V. Maroni, and M.V. Rane. High critical current YBCO films prepared by an MOD process on RABiTS templates. *IEEE Transactions on Applied Superconductivity*, 17(2):3553–3556, 2007.
- [15] D. M. Feldmann, T. G. Holesinger, R. Feenstra, C. Cantoni, W. Zhang, M. Rupich, X. Li, J. H. Durrell, A. Gurevich, and D. C. Larbalestier. Mechanisms for enhanced supercurrent across meandered grain boundaries in high-temperature superconductors. *Journal of Applied Physics*, 102(8):083912, 2007.
- [16] J. Eickemeyer, D. Selbmann, R. Huhne, H. Wendrock, J. Hanisch, A. Guth, L. Schultz, and B. Holzapfel. Elongated grains in textured substrate tapes and their effect on transport currents in superconductor layers. *Applied Physics Letters*, 90(1):012510, 2007.
- [17] B. A. Glowacki, M. E. Vickers, N. A. Rutter, E. Maher, F. Pasotti, A. Baldini, and R. Major. Texture development in long lengths of NiFe tapes for superconducting coated conductor. *Journal Of Materials Science*, 37(1):157–168, 2002.
- [18] A. Goyal, D. P. Norton, J. D. Budai, M. Paranthaman, E. D. Specht, D. M. Kroeger, D. K. Christen, Q. He, B. Saffian, F. A. List, D. F. Lee, P. M. Martin, C. E. Klabunde, E. Hartfield, and V. K. Sikka. High critical current density superconducting tapes by epitaxial deposition of  $\text{YBa}_2\text{Cu}_3\text{O}_7$  thick films on biaxially textured metals. *Applied Physics Letters*, 69(12):1795–1797, 1996.
- [19] A. Goyal, E. D. Specht, Z. L. Wang, and D. M. Kroeger. Grain boundary studies of high-temperature superconducting materials using electron backscatter Kikuchi diffraction. *Ultramicroscopy*, 67(1-4):35–57, 1997.
- [20] R. Nast, B. Obst, and W. Goldacker. Cube-textured nickel and Ni alloy substrates for YBCO coated conductors. *Physica C-Superconductivity And Its Applications*, 372:733–737, 2002.
- [21] A. Goyal, S. X. Ren, E. D. Specht, D. M. Kroeger, R. Feenstra, D. Norton, M. Paranthaman, D. F. Lee, and D. K. Christen. Texture formation and grain boundary networks in rolling assisted biaxially textured substrates and in epitaxial ybco films on such substrates. *Micron*, 30(5):463–478, 1999.
- [22] M. W. Rupich, W. Zhang, X. Li, T. Kodenkandath, D. T. Verebelyi, U. Schoop, C. Thieme, M. Teplitsky, J. Lynch, N. Nguyen, E. Siegal, J. Scudiere, V. Maroni, K. Venkataraman, D. Miller, and T. G. Holesinger. Progress on MOD/RABITS (tm) 2G hts wire. *Physica C-Superconductivity And Its Applications*, 412-14:877–884, 2004.
- [23] E. D. Specht, F. A. List, D. F. Lee, K. L. More, A. Goyal, W. B. Robbins, and D. O’Neill. Uniform texture in meter-long  $\text{YBa}_2\text{Cu}_3\text{O}_7$  tape. *Physica C-Superconductivity And Its Applications*, 382(2-3):342–348, 2002.
- [24] D. M. Feldmann, J. L. Reeves, A. A. Polyanskii, G. Kozlowski, R. R. Biggers, R. M. Nekkanti, I. Maartense, M. Tomsic, P. Barnes, C. E. Oberly, T. L. Peterson, S. E. Babcock, and D. C. Larbalestier. Influence of nickel substrate grain structure on  $\text{YBa}_2\text{Cu}_3\text{O}_7$  supercurrent connectivity in deformation-textured coated conductors. *Applied Physics Letters*, 77(18):2906–2908, 2000.
- [25] J. D. Budai, W. G. Yang, N. Tamura, J. S. Chung, J. Z. Tischler, B. C. Larson, G. E. Ice, C. Park, and D. P. Norton. X-ray microdiffraction study of growth modes and crystallographic tilts in oxide films on metal substrates. *Nature Materials*, 2(7):487–492, 2003.
- [26] N.A. Rutter and B.A. Glowacki. Modelling of orientation relations in 2-D percolative systems of buffered metallic substrates for coated conductors. *IEEE Transactions on Applied Superconductivity*, 11(1):2730–2733, 2001.
- [27] D. M. Feldmann, T. G. Holesinger, C. Cantoni, R. Feenstra, N. A. Nelson, D. C. Larbalestier, D. T. Verebelyi, X. Li, and M. Rupich. Grain orientations and grain boundary networks of  $\text{YBa}_2\text{Cu}_3\text{O}_7$  films deposited by metalorganic and pulsed laser deposition on biaxially textured Ni-W substrates. *Journal of Materials Research*, 21(4):923–934, 2006.
- [28] D. M. Feldmann, D. C. Larbalestier, T. Holesinger, R. Feenstra, A. A. Gapud, and E. D. Specht. Evidence for extensive grain boundary meander and overgrowth of substrate grain boundaries in high critical current density ex situ  $\text{YBa}_2\text{Cu}_3\text{O}_7$  coated conductors. *Journal of Materials Research*, 20(8):2012–2020, 2005.
- [29] S. Kang, A. Goyal, K. J. Leonard, N. A. Rutter, D. F. Lee, D. M. Kroeger, and M. P. Paranthaman. High critical current  $\text{YBa}_2\text{Cu}_3\text{O}_7$  thick films on improved rolling-assisted biaxially textured substrates (RABiTS (TM)). *Journal Of The American Ceramic Society*, 88(10):2677–2680, 2005.
- [30] L. Fernandez, B. Holzapfel, F. Schindler, B. de Boer, A. Attenberger, J. Hanisch, and L. Schultz. Influence of the grain boundary network on the critical current of  $\text{YBa}_2\text{Cu}_3\text{O}_7$  films grown on biaxially textured metallic substrates. *Physical Review B*, 67(5):052503, 2003.
- [31] J. L. Reeves, D. M. Feldmann, C. Y. Yang, and D. C. Larbalestier. Current barriers in y-ba-cu-o coated conductors. *IEEE Transactions On Applied Superconductivity*, 11(1):3863–3867, 2001.
- [32] D. M. Feldmann, J. L. Reeves, A. A. Polyanskii, A. Goyal, R. Feenstra, D. F. Lee, M. Paranthaman, D. M. Kroeger, D. K. Christen, S. E. Babcock, and D. C. Larbalestier. Magneto-optical imaging of transport currents in  $\text{YBa}_2\text{Cu}_3\text{O}_7$  on RABiTS (TM). *IEEE Transactions On Applied Superconductivity*, 11(1):3772–3775, 2001.

- [33] C. Y. Yang, S. E. Babcock, A. Ichinose, A. Goyal, D. M. Kroeger, D. F. Lee, F. A. List, D. P. Norton, J. E. Mathis, M. Paranthaman, and C. Park. Microstructure of pulsed laser deposited  $\text{YBa}_2\text{Cu}_3\text{O}_7$  films on yttria-stabilized zirconia/CeO<sub>2</sub> buffered biaxially textured ni substrates. *Physica C-Superconductivity And Its Applications*, 377(3):333–347, 2002.
- [34] T. Haugan, P. N. Barnes, R. Wheeler, F. Meisenkothen, and M. Sumption. Addition of nanoparticle dispersions to enhance flux pinning of the  $\text{YBa}_2\text{Cu}_3\text{O}_7$  superconductor. *Nature*, 430(7002):867–870, 2004.
- [35] J. L. MacManus-Driscoll, S. R. Foltyn, Q. X. Jia, H. Wang, A. Serquis, B. Maiorov, L. Civale, Y. Lin, M. E. Hawley, M. P. Maley, and D. E. Peterson. Systematic enhancement of in-field critical current density with rare-earth ion size variance in superconducting rare-earth barium cuprate films. *Applied Physics Letters*, 84(26):5329–5331, 2004.
- [36] J. L. Macmanus-Driscoll, S. R. Foltyn, Q. X. Jia, H. Wang, A. Serquis, L. Civale, B. Maiorov, M. E. Hawley, M. P. Maley, and D. E. Peterson. Strongly enhanced current densities in superconducting coated conductors of  $\text{YBa}_2\text{Cu}_3\text{O}_7+\text{BaZrO}_3$ . *Nature Materials*, 3(7):439–443, 2004.
- [37] K. J. Leonard, A. Goyal, D. M. Kroeger, J. W. Jones, S. Kang, N. Rutter, M. Paranthaman, D. F. Lee, and B. W. Kang. Thickness dependence of microstructure and critical current density of  $\text{YBa}_2\text{Cu}_3\text{O}_7$  on rolling-assisted biaxially textured substrates. *Journal Of Materials Research*, 18(5):1109–1122, 2003.
- [38] T. G. Holesinger, P. N. Arendt, R. Feenstra, A. A. Gapud, E. D. Specht, D. M. Feldmann, and D. C. Larbalestier. Liquid mediated growth and the bimodal microstructure of  $\text{YBa}_2\text{Cu}_3\text{O}_7$  films made by the ex situ conversion of physical vapor deposited  $\text{BaF}_2$  precursors. *Journal Of Materials Research*, 20(5):1216–1233, 2005.
- [39] X. F. Zhang, D. J. Miller, and J. Talvacchio. Control of meandering grain boundary configurations in  $\text{YBa}_2\text{Cu}_3\text{O}_7$  bicrystal thin films based on deposition rate. *Journal Of Materials Research*, 11(10):2440–2449, October 1996.
- [40] M. W. Rupich, U. Schoop, D. T. Verebelyi, C. Thieme, W. Zhang, X. Li, T. Kodenkandath, N. Nguyen, E. Siegal, D. Buczek, J. Lynch, M. Jowett, E. Thompson, J. S. Wang, J. Scudiere, A. P. Malozemoff, Q. Li, S. Annarapu, S. Cui, L. Fritzeimer, B. Aldrich, C. Craven, F. Niu, R. Schwall, A. Goyal, and M. Paranthaman. Ybco coated conductors by an MOD/RABiTS (TM) process. *IEEE Transactions on Applied Superconductivity*, 13(2):2458–2461, 2003.
- [41] T. G. Holesinger, L. Civale, B. Maiorov, D. M. Feldmann, J. Y. Coulter, J. Miller, V. A. Maroni, Z. J. Chen, D. C. Larbalestier, R. Feenstra, X. P. Li, M. B. Huang, T. Kodenkandath, W. Zhang, M. W. Rupich, and A. P. Malozemoff. Progress in nanoengineered microstructures for tunable high-current, high-temperature superconducting wires. *Advanced Materials*, 20(3):391–407, February 2008.
- [42] X. Li, M. W. Rupich, W. Zhang, N. Nguyen, T. Kodenkandath, U. Schoop, D. T. Verebelyi, C. Thieme, M. Jowett, P. N. Arendt, S. R. Foltyn, T. G. Holesinger, T. Aytug, D. K. Christen, and M. P. Paranthaman. High critical current mod ex situ ybco films on RABiTS (TM) and MgO-IBAD templates. *Physica C-Superconductivity And Its Applications*, 390(3):249–253, 2003.
- [43] Y. Kitoha, J. Matsudaa, K. Suzukia, R. Teranishia, K. Nakaokaa, Y. Aokia, H. Fujid, A. Yajimab, Y. Yamadac, T. Izumia and Y. Shiohara. Fabrication of  $\text{Y}_{1-x}\text{RE}_x\text{Ba}_2\text{Cu}_3\text{O}_y$  films on single crystalline substrates and IBAD buffered metallic tapes by advanced TFA-MOD process. *Physica C: Superconductivity*, 19(9):968–979, 2006.
- [44] S. I. Kim, A. Gurevich, X. Song, X. Li, W. Zhang, T. Kodenkandath, M. W. Rupich, T. G. Holesinger, and D. C. Larbalestier. Mechanisms of weak thickness dependence of the critical current density in strong-pinning ex situ metal-organic-deposition-route  $\text{YBa}_2\text{Cu}_3\text{O}_7$  coated conductors. *Superconductor Science & Technology*, 445(S1):558–562, 2006.
- [45] E. D. Specht, A. Goyal, and W. Liu. Local epitaxy of  $\text{YBa}_2\text{Cu}_3\text{O}_7$  on polycrystalline Ni measured by X-ray microdiffraction. *Journal Of Materials Research*, 22(3):664–674, 2007.
- [46] A. Kursumovic, J. E. Evetts, J. L. MacManus-Driscoll, B. Maiorov, L. Civale, H. Wang, Q. X. Jia, and S. R. Foltyn. High critical current densities in  $\text{YBa}_2\text{Cu}_3\text{O}_7$  films grown at high rates by hybrid liquid phase epitaxy. *Applied Physics Letters*, 87(25):252507, 2005.
- [47] Y. Xu, A. Goyal, J. Lian, N. A. Rutter, I. Shi, S. Sathyamurthy, M. Paranthaman, L. Wang, P. M. Martin, and D. M. Kroeger. Preparation of ybco films on CeO<sub>2</sub>-buffered (001) YSZ substrates by a non-fluorine mod method. *Journal Of The American Ceramic Society*, 87(9):1669–1676, 2004.
- [48] Y. Xu, A. Goyal, N. A. Rutter, D. Shi, M. Paranthaman, S. Sathyamurthy, P. M. Martin, and D. M. Kroeger. Fabrication of high-critical current density  $\text{YBa}_2\text{Cu}_3\text{O}_7$  films using a fluorine-free sol gel approach. *Journal Of Materials Research*, 18(3):677–681, 2003.
- [49] R. P. Reade, P. Berdahl, R. E. Russo, and S. M. Garrison. Laser deposition of biaxially textured yttria-stabilized zirconia buffer layers on polycrystalline metallic alloys for high critical current Y-Ba-Cu-O thin-films. *Applied Physics Letters*, 61(18):2231–2233, 1992.
- [50] J.R. Groves, P.N. Arendt, H. Kung, S.R. Foltyn, R.F. DePaula, L.A. Emmert, and J.G. Storer. Texture development in IBAD MgO films as a function of deposition thickness and rate. *IEEE Transactions on Applied Superconductivity*, 11(1):2822–2825, 2001.

- [51] L.S. Yu, J.M.E. Harper, J.J. Cuomo, and D.A. Smith. Alignment of thin-films by glancing angle ion-bombardment during deposition. *Applied Physics Letters*, 47(9):932–933, 1985.
- [52] J.R. Groves, P.N. Arendt, S.R. Foltyn, Q.X. Jia, T.G. Holesinger, H. Kung, R.F. DePaula, P.C. Dowden, E.J. Peterson, L. Stan, and L.A. Emmert. Recent progress in continuously processed IBAD MgO template meters for HTS applications. *Physica C-Superconductivity and Its Applications*, 382(1):43–47, 2002.
- [53] M. Paranthaman, T. Aytug, A. Goyal, and V. Selvamanickam. Ornl-superpower crada: Development of mocvd-based, ibad-2g wire, superconductivity for electric systems 2007 annual peer review, 2007.
- [54] R. Huhne, C. Beyer, B. Holzapfel, C.G. Oertel, L. Schultz, and W. Skrotzki. Growth of biaxial textured MgO-layers by ion-beam assisted pulsed laser deposition. *Crystal Research and Technology*, 35(4):419–425, 2000.
- [55] U. Balachandran and B. Ma. Fabrication of YBCO-coated conductors by inclined substrate deposition technique, superconductivity for electric systems 2002 annual peer review, 2002.
- [56] U. Balachandran, B. Ma, M. Li, B.L. Fisher, R.E. Koritala, D.J. Miller, and S.E. Dorris. Development of coated conductors by inclined substrate deposition. *Physica C-Superconductivity and Its Applications*, 392:806–814, 2003.
- [57] W. Prusseit, C. Hoffmann, R. Nemetschek, G. Sigl, J. Handke, A. Lumkemann, and H. Kinder. Reel to reel coated conductor fabrication by evaporation. *IEEE Transactions on Applied Superconductivity*, 16(2):996–998, 2006.
- [58] W. Prusseit, R. Nemetschek, C. Hoffmann, G. Sigl, A. Lumkemann, and H. Kinder. ISD process development for coated conductors. *Physica C-Superconductivity and Its Applications*, 426:866–871, 2005.
- [59] Y. Lin, H. Wang, B. Maiorov, M.E. Hawley, C.J. Wetteland, P.N. Arendt, S.R. Foltyn, L. Civale, and Q.X. Jia. Comparative study of microstructural properties for  $\text{YBa}_2\text{Cu}_3\text{O}_7$  films on single-crystal and Ni-based metal substrates. *Journal of Materials Research*, 20(8):2055–2060, 2005.
- [60] T.G. Holesinger, S.R. Foltyn, P.N. Arendt, H. Kung, Q.X. Jia, R.M. Dickerson, P.C. Dowden, R.F. DePaula, J.R. Groves, and J.Y. Coulter. The microstructure of continuously processed  $\text{YBa}_2\text{Cu}_3\text{O}_7$  coated conductors with underlying  $\text{CeO}_2$  and ion-beam-assisted yttria-stabilized zirconia buffer layers. *Journal of Materials Research*, 15(5):1110–1119, 2000.
- [61] S.R. Foltyn, Q.X. Jia, P.N. Arendt, L. Kinder, Y. Fan, and J.F. Smith. Relationship between film thickness and the critical current of  $\text{YBa}_2\text{Cu}_3\text{O}_7$  coated conductors. *Applied Physics Letters*, 75(23):3692–3694, 1999.
- [62] D. M. Feldmann, D. C. Larbalestier, R. Feenstra, A. A. Gapud, J. D. Budai, T. G. Holesinger, and P. N. Arendt. Through-thickness superconducting and normal-state transport properties revealed by thinning of thick film ex situ  $\text{YBa}_2\text{Cu}_3\text{O}_7$  coated conductors. *Applied Physics Letters*, 83(19):3951–3953, 2003.
- [63] V. Selvamanickam, G. Carota, M. Funk, N. Vo, P. Haldar, U. Balachandran, M. Chudzik, P. Arendt, J.R. Groves, R. DePaula, and B. Newnam. High-current Y-Ba-Cu-O coated conductor using metal organic chemical-vapor deposition and ion-beam-assisted deposition. *IEEE Transactions on Applied Superconductivity*, 11(1):3379–3381, 2001.
- [64] M.S. Hatzistergos, H. Efstathiadis, J.L. Reeves, V. Selvamanickam, L.P. Allen, E. Lifshin, and P. Haldar. Microstructural and compositional analysis of  $\text{YBa}_2\text{Cu}_3\text{O}_7$  films grown by MOCVD before and after GCIB smoothing. *Physica C-Superconductivity and Its Applications*, 405(3-4):179–186, 2004.
- [65] N. F. Heinig, R. D. Redwing, J. E. Nordman, and D. C. Larbalestier. Strong to weak coupling transition in low misorientation angle thin film  $\text{YBa}_2\text{Cu}_3\text{O}_7$  bicrystals. *Physical Review B*, 60(2):1409–1417, 1999.
- [66] P. Chaudhari, R. H. Koch, R. B. Laibowitz, T. R. McGuire, and R. J. Gambino. Critical-current measurements in epitaxial-films of  $\text{YBa}_2\text{Cu}_3\text{O}_7$  compound. *Physical Review Letters*, 58(25):2684–2686, 1987.
- [67] P. Chaudhari, J. Mannhart, D. Dimos, C. C. Tsuei, J. Chi, M. M. Oprysko, and M. Scheuermann. Direct measurement of the superconducting properties of single grain-boundaries in  $\text{YBa}_2\text{Cu}_3\text{O}_7$ . *Physical Review Letters*, 60(16):1653–1656, 1988.
- [68] A. DiChiara, F. Lombardi, F. M. Granozio, U. S. diUccio, F. Tafuri, and M. Valentino.  $\text{YBa}_2\text{Cu}_3\text{O}_7$  grain boundary josephson junctions with a MgO seed layer. *IEEE Transactions On Applied Superconductivity*, 7(2):3327–3330, June 1997.
- [69] D. T. Verebelyi, D. K. Christen, R. Feenstra, C. Cantoni, A. Goyal, D. F. Lee, M. Paranthaman, P. N. Arendt, R. F. DePaula, J. R. Groves, and C. Prouteau. Low angle grain boundary transport in  $\text{YBa}_2\text{Cu}_3\text{O}_7$  coated conductors. *Applied Physics Letters*, 76(13):1755–1757, 2000.
- [70] D. T. Verebelyi, C. Cantoni, J. D. Budai, D. K. Christen, H. J. Kim, and J. R. Thompson. Critical current density of  $\text{YBa}_2\text{Cu}_3\text{O}_7$  low-angle grain boundaries in self-field. *Applied Physics Letters*, 78(14):2031–2033, 2001.
- [71] T. Horide, K. Matsumoto, Y. Yoshida, M. Mukaida, A. Ichinose, and S. Horii. Tilt angle dependences of vortex structure and critical current density at low-angle grain boundaries in  $\text{YBa}_2\text{Cu}_3\text{O}_7$  films. *Physical Review B*, 77(13):132502, 2008.
- [72] A. Diaz, L. Mechin, P. Berghuis, and J. E. Evetts. Observation of viscous flux flow in  $\text{YBa}_2\text{Cu}_3\text{O}_7$  low-angle grain boundaries. *Physical Review B-Condensed Matter*, 58(6):R2960–R2963, 1998.
- [73] J. E. Evetts, M. J. Hogg, B. A. Glowacki, N. A. Rutter, and V. N. Tsaneva. Current percolation and

- the v-i transition in  $\text{YBa}_2\text{Cu}_3\text{O}_7$  bicrystals and granular coated conductors. *Superconductor Science & Technology*, 12(12):1050–1053, 1999.
- [74] M. J. Hogg, F. Kahlmann, E. J. Tarte, Z. H. Barber, and J. E. Evetts. Vortex channeling and the voltage-current characteristics of  $\text{YBa}_2\text{Cu}_3\text{O}_7$  low-angle grain boundaries. *Applied Physics Letters*, 78(10):1433–1435, 2001.
- [75] A. Palau, T. Puig, X. Obradors, E. Pardo, C. Navau, A. Sanchez, A. Usoskin, H.C. Freyhardt, L. Fernandez, B. Holzapfel, and R. Feenstra. Simultaneous inductive determination of grain and intergrain critical current densities of  $\text{YBa}_2\text{Cu}_3\text{O}_7$  coated conductors. *Applied Physics Letters*, 84(2):230–232, 2004.
- [76] S. Tonies, A. Vostner, and H. W. Weber. Determination of inter- and intragranular currents in high temperature superconducting tapes and coated conductors. *Journal Of Applied Physics*, 92(5):2628–2633, September 2002.
- [77] J. R. Thompson, H. J. Kim, C. Cantoni, D. K. Christen, R. Feenstra, and D. T. Verebelyi. Self-organized current transport through low-angle grain boundaries in  $\text{YBa}_2\text{Cu}_3\text{O}_7$  thin films studied magnetometrically. *Physical Review B*, 69(10):104509, 2004.
- [78] A. A. Polyanskii, A. Gurevich, A. E. Pashitski, N. F. Heinig, R. D. Redwing, J. E. Nordman, and D. C. Larbalestier. Magneto-optical study of flux penetration and critical current densities in 001 tilt  $\text{YBa}_2\text{Cu}_3\text{O}_7$  thin-film bicrystals. *Physical Review B*, 53(13):8687–8697, 1996.
- [79] G. K. Perkins. Private correspondence.
- [80] T. Horide, K. Matsumoto, Y. Yoshida, M. Mukaida, A. Ichinose, and S. Horii. Combined effect of a single grain boundary and artificial pinning centers on the critical current density in a  $\text{YBa}_2\text{Cu}_3\text{O}_7$  thin film. *Applied Physics Letters*, 89(17):172505, 2006.
- [81] A. Gurevich, M. S. Rzechowski, G. Daniels, S. Patnaik, B. M. Hinaus, F. Carillo, F. Tafuri, and D. C. Larbalestier. Flux flow of Abrikosov-Josephson vortices along grain boundaries in high-temperature superconductors. *Physical Review Letters*, 88(9):097001, 2002.
- [82] A. Diaz, L. Mechin, P. Berghuis, and J. E. Evetts. Evidence for vortex pinning by dislocations in  $\text{YBa}_2\text{Cu}_3\text{O}_7$  low-angle grain boundaries. *Physical Review Letters*, 80(17):3855–3858, 1998.
- [83] J. E. Evetts and B. A. Glowacki. Relation of critical current irreversibility to trapped flux and microstructure in polycrystalline  $\text{YBa}_2\text{Cu}_3\text{O}_7$ . *Cryogenics*, 28(10):641–649, October 1988.
- [84] A. A. Gapud, D. K. Christen, R. Feenstra, F. A. List, and A. Khan. On narrowing coated conductor film: the emergence of granularity-induced field hysteresis of transport critical current. *Superconductor Science & Technology*, 21(7):075016, July 2008.
- [85] J. H. Durrell, M. J. Hogg, F. Kahlmann, Z. H. Barber, M. G. Blamire, and J. E. Evetts. Critical current of  $\text{YBa}_2\text{Cu}_3\text{O}_7$  low-angle grain boundaries. *Physical Review Letters*, 90(24):247006, 2003.
- [86] T. Horide, K. Matsumoto, Y. Yoshida, M. Mukaida, A. Ichinose, and S. Horii. The limitation mechanism of  $j(c)$ - $\theta$  characteristics in  $\text{YBa}_2\text{Cu}_3\text{O}_7$  thin film with a single low angle grain boundary. *Physica C-Superconductivity And Its Applications*, 463:678–681, 2007.
- [87] M. F. Chisholm and S. J. Pennycook. Structural origin of reduced critical currents at  $\text{YBa}_2\text{Cu}_3\text{O}_7$  grain-boundaries. *Nature*, 351(6321):47–49, 1991.
- [88] R.B. Dinner, K.A. Moler, M.R. Beasley, and D.M. Feldmann. Enhanced current flow through meandering grain boundaries in  $\text{YBa}_2\text{Cu}_3\text{O}_7$  films. *Appl. Phys. Lett.*, 90(21):212501, 2007.
- [89] S. Leitenmeier, H. Bielefeldt, G. Hammerl, A. Schmehl, C. W. Schneider, and J. Mannhart. Coated conductors containing grains with big aspect ratios. *Annalen Der Physik*, 11(7):497–502, 2002.
- [90] G. Hammerl, A. Herringer, A. Schmehl, A. Weber, K. Wiedenmann, C.W. Schneider, and J. Mannhart. Possible solution of the grain-boundary problem for applications of high Tc superconductors. *Appl. Phys. Lett.*, 81(17):3209–3211, 2002.
- [91] G. Hammerl, H. Bielefeldt, S. Leitenmeier, A. Schmehl, A. Weber, C.W. Schneider, and J. Mannhart. Improving coated conductors. *IEEE Trans. Appl. Supercond.*, 13(2):2625–2627, 2003.
- [92] D. J. Miller, T. A. Roberts, J. H. Kang, J. Talvacchio, D. B. Buchholz, and R. P. H. Chang. Meandering grain-boundaries in  $\text{YBa}_2\text{Cu}_3\text{O}_7$  bi-crystal thin-films. *Applied Physics Letters*, 66(19):2561–2563, 1995.
- [93] C. Traeholt, J. G. Wen, V. Svetchnikov, and H. W. Zandbergen. HREM study of the YBCO MgO interface on an atomic-scale. *Physica C*, 230(3-4):297–305, 1994.
- [94] K. E. Gray, M. B. Field, and D. J. Miller. Explanation of low critical currents in flat, bulk versus meandering, thin-film [001] tilt bicrystal grain boundaries in  $\text{YBa}_2\text{Cu}_3\text{O}_7$ . *Physical Review B*, 58(14):9543–9548, 1998.
- [95] J. H. Durrell, D. M. Feldmann, and C. Cantoni. Suppression of vortex channeling in meandered  $\text{YBa}_2\text{Cu}_3\text{O}_7$  grain boundaries. *Applied Physics Letters*, 91(18):182506, 2007.
- [96] D. Abaimov, D. M. Feldmann, A. A. Polyanskii, A. Gurevich, G. Daniels, D. C. Larbalestier, A. P. Zhuravel, and A. V. Ustinov. Scanning laser imaging of dissipation in  $\text{YBa}_2\text{Cu}_3\text{O}_7$  coated conductors. *Applied Physics Letters*, 85(13):2568–2570, 2004.
- [97] N.A. Rutter and B.A. Glowacki. Modelling the V-I characteristic of coated conductors. *Supercond. Sci. Technol.*, 14(9):680–684, 2001.

- [98] S. I. Kim, D. M. Feldmann, D. T. Verebelyi, C. Thieme, X. Li, A. A. Polyanskii, and D. C. Larbalestier. Influence of the grain boundary network on the critical current density of deformation-textured  $\text{YBa}_2\text{Cu}_3\text{O}_7$  coated conductors made by metal-organic deposition. *Physical Review B*, 71(10):104501, 2005.
- [99] S. R. Foltyn, P. N. Arendt, Q. X. Jia, H. Wang, J. L. MacManus-Driscoll, S. Kreiskott, R. F. DePaula, L. Stan, J. R. Groves, and P. C. Dowden. Strongly coupled critical current density values achieved in  $\text{YBa}_2\text{Cu}_3\text{O}_7$  coated conductors with near-single-crystal texture. *Applied Physics Letters*, 82(25):4519–4521, 2003.
- [100] N. A. Rutter, J. H. Durrell, M. G. Blamire, J. L. MacManus-Driscoll, H. Wang, and S. R. Foltyn. Benefits of current percolation in superconducting coated conductors. *Applied Physics Letters*, 87(16):162507, 2005.
- [101] C. Jooss, R. Warthmann, A. Forkl, and H. Kronmüller. High-resolution magneto-optical imaging of critical currents in  $\text{YBa}_2\text{Cu}_3\text{O}_7$  thin films. *Physica C*, 299(3-4):215–230, 1998.
- [102] J. E. Evetts and A. M. Campbell. *Concise Encyclopedia of Magnetic and Superconducting Materials*, chapter Critical State Model, pages 95–101. Pergamon Press, 1992.
- [103] S. Furtner, R. Nemetschek, R. Semerad, G. Sigl, and W. Prusseit. Reel-to-reel critical current measurement of coated conductors. *Superconductor Science & Technology*, 17(5):S281–S284, May 2004.
- [104] D. C. van der Laan, M. Dhalle, L. M. Naveira, H. J. N. van Eck, A. Metz, J. Schwartz, M. W. Davidson, B. ten Haken, and H. J. ten Kate. Direct experimental analysis of the relation between the grain structure and the distribution of critical current density in  $\text{YBa}_2\text{Cu}_3\text{O}_7$  coated conductors. *Superconductor Science & Technology*, 18(3):299–306, March 2005.
- [105] A. Palau, T. Puig, X. Obradors, and C. Jooss. Simultaneous determination of grain and grain-boundary critical currents in  $\text{YBa}_2\text{Cu}_3\text{O}_7$ -coated conductors by magnetic measurements. *Phys. Rev. B*, 75(5):054517, 2007.
- [106] A. Palau, T. Puig, X. Obradors, R. Feenstra, A.A. Gapud, E.D. Specht, D.M. Feldmann, and T.G. Holesinger. Grain and grain-boundary critical currents in coated conductors with noncorrelating  $\text{YBa}_2\text{Cu}_3\text{O}_7$  and substrate grain-boundary networks. *Appl. Phys. Lett.*, 88(13):132508, 2006.
- [107] A. Palau, T. Puig, X. Obradors, R. Feenstra, and A.A. Gapud. Correlation between grain and grain-boundary critical current densities in ex situ coated conductors with variable  $\text{YBa}_2\text{Cu}_3\text{O}_7$  layer thickness. *Applied Physics Letters*, 88(12):122502, 2006.
- [108] T. Puig, A. Palau, X. Obradors, E. Pardo, C. Navau, A. Sanchez, C. Jooss, K. Guth, and H.C. Freyhardt. The identification of grain boundary networks of distinct critical current density in  $\text{YBa}_2\text{Cu}_3\text{O}_7$  coated conductors. *Supercond. Sci. Technol.*, 17(11):1283–1288, 2004.
- [109] E.D. Specht, A. Goyal, and D.M. Kroeger. Scaling of percolative current flow to long lengths in biaxially textured conductors. *Superconductor Science & Technology*, 13(5):592–597, 2000.
- [110] N.A. Rutter, B.A. Glowacki, and J.E. Evetts. Percolation modelling for highly aligned polycrystalline superconducting tapes. *Supercond. Sci. Technol.*, 13(11):L25–L30, 2000.
- [111] Y. Nakamura, T. Izumi, and Y. Shiohara. Percolation analysis of the effect of tape length on the critical current density of 123 coated conductors. *Physica C*, 371(4):275–284, 2002.
- [112] N.A. Rutter. *Microstructural Development and Superconducting Parameters of the  $\text{YBa}_2\text{Cu}_3\text{O}_7$  Coated Conductor*. PhD thesis, University of Cambridge 2001.
- [113] J. Hanisch, V.S. Sarma, B. Zeimetz, F. Schindler, J. Eickemeyer, L. Schultz, and B. Holzapfel. Simulation of the critical current density and its dependence on geometrical factors in rabbits based coated conductors. *Supercond. Sci. Technol.*, 17(8):1003–1008, 2004.
- [114] B. Holzapfel, L. Fernandez, F. Schindler, B. de Boer, N. Reger, J. Eickemeyer, P. Berberich, and W. Prusseit. Grain boundary networks in  $\text{Y}123$  coated conductors: Formation, properties and simulation. *IEEE Transactions on Applied Superconductivity*, 11(1):3872–3875, 2001.
- [115] N.A. Rutter and A. Goyal. In *High Temperature Superconductivity 1*, pages 377–400. Springer, Berlin, 2004.
- [116] A. Goyal, N. Rutter, C. Cantoni, and D.F. Lee. Long-range current flow and percolation in rabbits-type conductors and the relative importance of out-of-plane and in-plane misorientations in determining  $j(c)$ . *Physica C*, 426:1083–1090, 2005.
- [117] M. Frary and C.A. Schuh. Nonrandom percolation behavior of grain boundary networks in high- $T_c$  superconductors. *Appl. Phys. Lett.*, 83(18):3755–3757, 2003.
- [118] M. Frary and C.A. Schuh. Percolation and statistical properties of low- and high-angle interface networks in polycrystalline ensembles. *Phys. Rev. B*, 69(13):134115, 2004.
- [119] L.R. Ford and D.R. Fulkerson. A primal-dual algorithm for the capacitated hitchcock problem. *Naval Research Logistics Quarterly*, 4(1):47–54, 1957.
- [120] B. Zeimetz, N.A. Rutter, B.A. Glowacki, and J.E. Evetts. Computer simulation of current percolation in polycrystalline high-temperature superconductors. *Supercond. Sci. Technol.*, 14(9):672–675, 2001.
- [121] B.A. Glowacki, M. Majoros, N.A. Rutter, and A.M. Campbell. Superconducting-magnetic heterostructures as a new method of decreasing transport ac losses in multifilamentary and coated superconductors. *Cryogenics*, 41(2):103–109, 2001.
- [122] B. Zeimetz, B.A. Glowacki, and J.E. Evetts. Resistor network model for simulation of current and flux percolation in granular coated conductors. *Physica C*, 372:767–770, 2002.

- [123] T. Kiss, M. Inoue, S. Egashira, T. Kuga, M. Ishimaru, M. Takeo, T. Matsushita, Y. Iijima, K. Kakimoto, T. Saitoh, S. Awaji, K. Watanabe, and Y. Shiohara. Percolative transition and scaling of transport E-J characteristics in YBCO coated IBAD tape. *IEEE Trans. Appl. Supercond.*, 13(2):2607–2610, 2003.
- [124] Mike Hogg. *The Electronic Properties of Thin Film  $YBa_2Cu_3O_7$  Low Angle Grain Boundaries*. PhD thesis, University of Cambridge, 2002.
- [125] John Durrell. *Critical Current Anisotropy in High Temperature Superconductors*. PhD thesis, University of Cambridge, 2001.
- [126] J. H. Durrell, G. Burnell, Z. H. Barber, M. G. Blamire, and J. E. Evetts. Critical currents in vicinal YBCO films. *Physical Review B*, 70(21):214508, 2004.
- [127] J. H. Durrell, S. H. Mennema, C. Jooss, G. Gibson, Z. H. Barber, H. W. Zandbergen, and J. E. Evetts. Flux line lattice structure and behavior in antiphase boundary free vicinal  $YBa_2Cu_3O_7$  thin films. *Journal of Applied Physics*, 93(12):9869–9874, 2003.